Model analysis and data validation of structured prevention and control interruptions of emerging infectious diseases

Hao Zhou[a], He Sha[a], Robert A. Cheke[b], Sanyi Tang[a,*]

[a]School of Mathematics and Statistics, Shaanxi Normal University, Xi'an, 710062, P.R. China
[b]Natural Resources Institute, University of Greenwich at Medway, Central Avenue, Chatham Maritime, Kent, ME4 4TB, UK

Abstract

The design of optimized non-pharmaceutical interventions (NPIs) is critical to the effective control of emergent outbreaks of infectious diseases such as SARS, A/H1N1 and COVID-19 and to ensure that numbers of hospitalized cases do not exceed the carrying capacity of medical resources. To address this issue, we formulated a classic SIR model to include a close contact tracing strategy and structured prevention and control interruptions (SPCIs). The impact of the timing of SPCIs on the maximum daily number of non-isolated infected individuals and on the duration of an infectious disease outside quarantined areas (i.e. implementing a dynamic zero-case policy) were analyzed numerically and theoretically. These analyses revealed that to minimize the maximum number of non-isolated infected individuals, the optimal time to initiate SPCIs is when they can control the peak value of a second rebound of the epidemic to be equal to the first peak value. More individuals may be infected at the peak of the second wave with a stronger intervention during SPCIs. The longer the duration of the intervention and the stronger the contact tracing intensity during SPCIs, the more effective they are in shortening the duration of an infectious disease outside quarantined areas. The dynamic evolution of the number of isolated and non-isolated individuals, including two peaks and long tail patterns, have been confirmed by various real data sets of multiple-wave COVID-19 epidemics in China. Our results provide important theoretical support for the adjustment of NPI strategies in relation to a given carrying capacity of medical resources.

Keywords: Emerging infectious diseases, Structured prevention and control interruptions, Multiple peaks, Optimal strategy

1. Introduction

The COVID-19 pandemic has been continuing for more than two years, and during this period the causative virus has mutated constantly [1, 2]. From the original strain to the Delta strain, and then to the rapidly spreading Omicron strain, the infection rate is increasing and the generation time is shrinking [3, 4], adversely impacting the prevention and control of the various variants. Medical institutions are facing difficult situations as they must control secondary waves of transmission with increasing numbers of patients whilst simultaneously treating critically ill patients. The quality of medical care deteriorates rapidly, especially when the number of infected patients exceeds the capacity of medical resources and the number of medical devices required for life support reaches a limit, thereby increasing the fatality rate [5, 6]. To mitigate the spread of sudden outbreaks of infectious diseases including SARS, A/H1N1 and COVID-19, non-pharmaceutical interventions (NPIs) [7–10], including case isolation, voluntary home quarantine, case isolation, voluntary home quarantine, closures of schools and universities, social distancing, prevention of mass gatherings, protective mask wearing and border closures have all played important roles.

*Corresponding author
Email address: sytang@snnu.edu.cn (Sanyi Tang)

However, long-term implementation of NPIs is not only difficult to sustain, but also challenges normal social life and economic development [11], so it is critically important to design optimized NPIs to effectively control an epidemic [12, 13]. On the other hand, stresses on the capacity of medical resources and other factors have led to the emergence of a complex switching and mixing mode of different NPI strategies to strengthen the prevention and control of emergent infectious diseases such as SARS, A/H1N1 and COVID-19 throughout the world [14]. Such switches in prevention and control modes in turn stimulate changes in epidemic outcomes to some extent. Thus, two key questions arise: (1) how to design strategies of structured prevention and control interruptions (SPCIs) to implement NPIs in the course of a dynamically evolving epidemic? and (2) how to obtain single or multi-objective optimal control schemes to delay and reduce the magnitude of peak numbers of cases, reduce the final overall size of an epidemic, shorten the time for its eradication and ensure that the number of hospitalized cases does not exceed the carrying capacity of medical resources?

Mathematical models can contribute to further understanding of these phenomena by obtaining analytical solutions as well as providing numerical simulations. SPCIs offer an alternative to continuous intervention by alternating between on and off cycles of intervention in order to enhance their utility and relieve the social and economic pressures that they impose. The impacts of SPCIs on disease control are evaluated here as a discontinuous change of parameters in the mathematical model. The simplest case based on the basic SIR model, in which an intervention is implemented (or strengthened) only once during an epidemic, i.e. a one-shot intervention model, has been widely studied both numerically [15, 16] and theoretically [17]. For example, Lauro and Kiss et al [15] numerically investigated the dependence of the final size and the peak fraction of infected individuals on the timing of a one-shot intervention during an epidemic, and showed that to minimise the peak fraction of infected individuals, the optimal time to introduce the intervention is when the current peak fraction is equal to the peak fraction that would occur once the disease rebounds. Bootsma and Ferguson [16] showed with numerical simulations that the final size of the number of infected individuals depended on the timing of the one-shot intervention, and that it can be minimized for weaker interventions with larger control reproduction numbers. Nacya and Tomokatsu et al [17] focused on the quantitative relationship between the strength of a one-shot intervention and the reduction in the number of infected individuals.

As the COVID-19 epidemic continues, a series of strict prevention and control measures have been implemented, including close contact tracing, quarantining of individuals with suspected infection, immigrant monitoring, etc. Close contact tracing has been commonly considered as an effective measures to interrupt further transmission of the epidemic [18, 19]. For modelling the implementation of close contact tracing, the SIR epidemiological models have been extensively developed [20–22]. For example, the infected population is further divided into non-isolated infected (I) and isolated infected (I_q) compartments. However, in the basic SIR epidemiological model [15–17], the population is only divided into susceptible (S), infected (I) and recovered (R) compartments. It is difficult to analyze the effect of the close contact tracing strategy on epidemic prevention and control. One of the aims of our work is to investigate the effects of close contact tracing strategies. On the other hand, the spread of infection is mainly caused by infected individuals who are not isolated or traced, including asymptomatic infected individuals who are less likely to be detected and difficult to trace. In [23], Fraser and Riley et al discussed the effect of asymptomatic transmission on the outbreak, and revealed that it is the key for control. In regular epidemic prevention and control of COVID-19, removing non-isolated infected individuals means that the infectious disease will be eradicated outside quarantined areas, thereby realizing the dynamic zero-case policy [24, 25]. Thus, it is essential to investigate the dynamic evolution of the non-isolated infected individuals during the dynamic evolution of the overall epidemic.

In this study, we consider an SIR-type epidemiological model with close contact tracing strategies involving SPCIs. In particular, we aim to analyze the impact of the timing of SPCIs and the intensity of the close contact tracing strategy on the maximum number of non-isolated infected individuals and the time needed to realize the dynamic zero-case. We also investigate optimal strategies for implementing SPCIs that minimize the maximum number of non-isolated infected individuals and the time needed to realize the dynamic zero-case policy. To confirm the main results and their implications, we use real data sets on COVID-19 in China to identify the unknown parameters and reveal the importance of SPCIs during the disease control procedures. So, the multiple

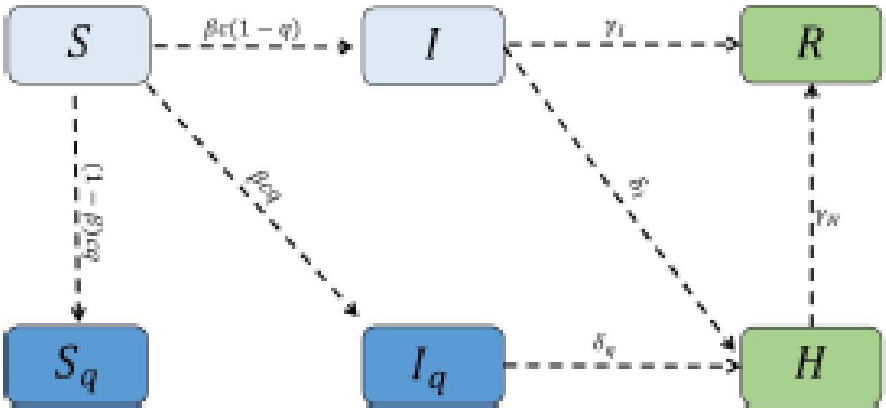

Figure 1: Diagram of the model adopted for simulating the epidemic. For explanations of state variables and parameters see text describing equation (2.1).

theoretical results presented by the model can be evaluated against data on multiple waves of COVID-19 epidemics.

2. Model

2.1. An SIR model with a close contact tracing strategy

In order to describe the close contact tracing and isolation measures taken by China for the prevention and control of COVID-19, we adopt the basic model idea proposed by Keeling and Rohani [26], for which the flow diagram is given in Fig.1. To formulate the model, we classify the population as susceptible (S), quarantined susceptible (S_q), non-isolated infected (I), isolated infected (I_q), hospitalized (H) and recovered (R) compartments, where the non-isolated infected population (I) includes asymptomatic infected individuals which are difficult to trace and detect. Further, we denote the contact tracing ratio as q, which indicates that the traced population will be quarantined or isolated, depending on whether they are infected or not. Meanwhile, the untraced population (a ratio $1-q$) consisting of individuals exposed to the virus who are missed from the contact tracing, will stay in the S_q compartment if they are not infected or move to I if they are infected. The untraced infected individuals can be detected and then move to the compartment H at a rate δ_I. Let δ_q be the diagnosis rate for individuals in compartment I_q, who will become hospitalized. Note that non-isolated infected individuals may also recover naturally, so the model requires a transition from I to R. γ_I is the natural recovery rate for individuals in compartment I and γ_H is the removal rate of hospitalized individuals in compartment H. Therefore, the transmission dynamics are governed by the following system:

$$\begin{cases} \dfrac{dS(t)}{dt} = -\dfrac{\beta c + cq(1-\beta)}{N} S(t)I(t), \\ \dfrac{dI(t)}{dt} = \dfrac{\beta c(1-q)}{N} S(t)I(t) - \delta_I I(t) - \gamma_I I(t), \\ \dfrac{dS_q(t)}{dt} = \dfrac{(1-\beta)cq}{N} S(t)I(t), \\ \dfrac{dI_q(t)}{dt} = \dfrac{\beta cq}{N} S(t)I(t) - \delta_q I_q(t), \\ \dfrac{dH(t)}{dt} = \delta_q I_q(t) + \delta_I I(t) - \gamma_H H(t), \\ \dfrac{dR(t)}{dt} = \gamma_H H(t) + \gamma_I I(t), \end{cases} \tag{2.1}$$

where we denote the transmission probability to be β and the contact rate as c. Due to the short duration of each epidemic wave that occurred in mainland China after the Wuhan epidemic in 2020-2022 [27], the corresponding

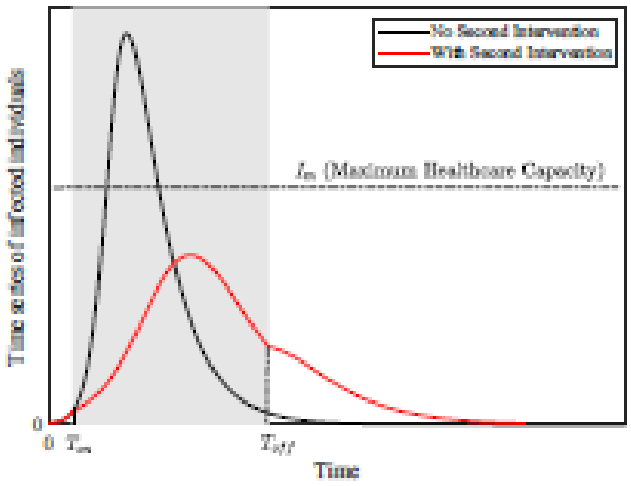

Figure 2: The time series of infected individuals with a second intervention, where the second intervention is implemented when $T_{on} \le t \le T_{off}$. I_m represents the maximum healthcare capacity during an infectious disease outbreak.

changes in the behaviour of the recovered individuals and given that antibodies raised in recovered individuals against COVID-19 provide protection for at least several weeks following infection, immediate reinfection with the virus is unlikely [28]. In our model, we do not consider the return of recovered individuals (R) to the free susceptible compartment (S).

2.2 *Structured prevention and control interruptions*

How to design the SPCI strategies to reduce the maximum number of non-isolated infections and shorten the period needed to realize dynamic zero-case aim is crucial for controlling multiple peaks of infectious diseases such as the COVID-19 epidemics that have occurred in mainland China and elsewhere. To address these key issues, we introduce the effect of SPCIs on disease control into the contact rate c and the quarantine rate q, i.e., a discontinuous change of the contact rate c and the quarantine rate q in a model to represent temporal discontinuities in the prevention and control measures. Here we also consider the simple case of SPCIs, where the intervention is strengthened (or implemented) only once during the epidemic. The fixed one-shot intervention is determined by the start time T_{on} and the end time T_{off}, and consequently the process of dynamic evolution of the overall epidemic situation is divided into three stages (as shown in Fig.2), as follows:

- Regular epidemic prevention and control stage ($t \le T_{on}$);
- Enhanced epidemic prevention and control (termed the second intervention) stage ($T_{on} < t \le T_{off}$);
- Regular epidemic prevention and control stage ($t > T_{off}$).

Correspondingly, we let $c = c_0$ and $q = q_0$ be the basic values for the contact and quarantine rates, respectively, during the regular epidemic prevention and control. They are switched to $c = c_c$ and $q = q_c$ once the intervention is strengthened (or the second intervention is implemented) at $t = T_{on}$, and restored to $c = c_0$ and $q = q_0$ at $t = T_{off}$, respectively. Therefore, a discontinuous control scheme acting on system (2.1) can be formulated as follows:

$$c = \begin{cases} c_0, & t \le T_{on}, \\ c_c, & T_{on} < t \le T_{off}, \\ c_0, & t > T_{off}, \end{cases} \quad \text{and} \quad q = \begin{cases} q_0, & t \le T_{on}, \\ q_c, & T_{on} < t \le T_{off}, \\ q_0, & t > T_{off}. \end{cases} \tag{2.2}$$

In this paper, we will focus on the dependence of the maximum number of non-isolated infected individuals and the time needed to realize the dynamic zero-case policy on the timing of the second intervention and the intensity of the close contact tracing strategy, and provide quantitative relationships with no approximation.

3. Preliminaries

In this section, we initially give some preliminary results of system (2.1). Note that the recovered R, hospitalized H, quarantined susceptible S_q and isolated infected I_q compartments are decoupled from the first two equations in (2.1), so we only need to consider the following two-dimensional system

$$\begin{cases} \dfrac{dS(t)}{dt} = -\beta_1 S(t)I(t), \\ \dfrac{dI(t)}{dt} = \beta_2 S(t)I(t) - \gamma I(t), \end{cases} \tag{3.1}$$

where $\beta_1 = \frac{\beta c + cq(1-\beta)}{N}$, $\beta_2 = \frac{\beta c(1-q)}{N}$, $\gamma = \delta_I + \gamma_I$ and $\beta_1 > \beta_2$ due to the isolation measures. By using the next generation matrix method, we can obtain that the basic reproduction number is $R_0 = \frac{\beta_2 S_0}{\gamma}$ and the effective reproduction number is $R_e = \frac{\beta_2 S(t)}{\gamma}$. Solving the above equation with initial value (S_0, I_0) yields the following first integral

$$I(t) + \frac{\beta_2}{\beta_1} S(t) - \rho_1 \ln(S(t)) = I_0 + \frac{\beta_2}{\beta_1} S_0 - \rho_1 \ln(S_0), \tag{3.2}$$

where $\rho_1 = \frac{\gamma}{\beta_1}$. Substituting it into the first equation of model (3.1), we have

$$S' = -\beta_1 S \left[-\frac{\beta_2}{\beta_1} S(t) + \rho_1 \ln(S(t)) + I_0 + \frac{\beta_2}{\beta_1} S_0 - \rho_1 \ln(S_0) \right] \doteq SF(S), \tag{3.3}$$

where

$$F(S) = \beta_2 S(t) - \beta_1 \rho_1 \ln(S(t)) - \beta_1 I_0 - \beta_2 S_0 + \beta_1 \rho_1 \ln(S_0).$$

By a simple calculation, we have

$$F'(S) = \beta_2 - \beta_1 \rho_1 \frac{1}{S}.$$

Solving $F'(S) = 0$ yields the extreme point $S_{min} \doteq \frac{\gamma}{\beta_2} = \frac{\beta_1 \rho_1}{\beta_2} > 0$. Moreover, it is easy to see that if $0 < S < S_{min}$ then $F'(S) < 0$; If $S > S_{min}$ then $F'(S) > 0$, which indicates that the function $F(S)$ reaches a minimal value at $S = S_{min}$. Further, we have $\lim_{S \to 0} F(S) = +\infty$ and $F(S_0) = -\beta_1 I_0 < 0$. Thus, the equation $F(S) = 0$ has a unique positive root in the interval $S \in (0, S_0)$, denoted as S_*. This indicates that there is a unique non-trivial equilibrium S_* for system (3.3).

For system (3.3), it is easy to verify that the zero equilibrium is unstable. And we can further show that the function $F(S)$ satisfies the following properties: $S' > 0$ for all $0 < S < S_*$, and $S' < 0$ for all $S_* < S < S_0$. Therefore, the unique equilibrium of system (3.3) is globally asymptotically stable. It follows from the relation

$$I(t) + \frac{\beta_2}{\beta_1} S(t) - \rho_1 \ln(S(t)) = I_0 + \frac{\beta_2}{\beta_1} S_0 - \rho_1 \ln(S_0)$$

and the formula for S_* that the limitation $\lim_{t \to +\infty} S(t) = S_*$ must imply the limitation $\lim_{t \to +\infty} I(t) = 0$, which confirms that the disease free equilibrium $(S_*, 0)$ of model (3.1) is globally stable. According to the equation $F(S) = 0$ and the properties of the *Lambert W* function we have

$$S_* = -\frac{\beta_1 \rho_1}{\beta_2} Lambert\, W \left[0, -\frac{\beta_2}{\beta_1 \rho_1} e^{-\frac{I_0 + \frac{\beta_2}{\beta_1} S_0 - \rho_1 \ln(S_0)}{\rho_1}} \right] < S_{min}$$

and

$$S^* = -\frac{\beta_2\rho_1}{\beta_1}Lambert\,W\left[-1, -\frac{\beta_1}{\beta_1\rho_1}e^{-\frac{I_0+\frac{\beta_2}{\beta_1}S_0-\rho_1\ln(S_0)}{\rho_1}}\right] > S_{min}.$$

This means that we obtain the analytical formula for the unique equilibrium S_*. Further, if $\beta_1 = \beta_2$ and the total number of individuals in the population is a constant N, then the final size satisfies $\lim_{t\to+\infty} R(t) = N - S_*$ in system (2.1).

Remark 3.1. *Note that for system (3.1), it is easy to verify that $I(+\infty) = 0$, i.e. there is no finite value T_{end} such that $I(T_{end}) = 0$ if $I(t)$ denotes the number of non-isolated infected individuals. In fact, we know that if the number of non-isolated infected individuals decreases and is less than 1, then the infectious disease will be eradicated outside quarantined areas when there is no infection reintroduced into the population. Therefore, we suppose that the infectious disease will be eradicated outside quarantined areas (i.e. realizing the dynamic zero-case policy) at $t = T_{end}$ provided that $I'(T_{end}) < 0$ and $I(T_{end}) = 1$.*

4. Analysis

In this section, we discuss the dynamical behaviour of system (2.1) with (2.2), which is equivalent to the following system

$$\begin{cases} \dfrac{dS(t)}{dt} = -\beta_1 S(t)I(t), \\ \dfrac{dI(t)}{dt} = \beta_2 S(t)I(t) - \gamma I(t) \end{cases} \tag{4.1}$$

with

$$\beta_1 = \begin{cases} \beta_{10}, & t \le T_{on}, \\ \beta_{1c}, & T_{on} < t \le T_{off}, \\ \beta_{10}, & t > T_{off}, \end{cases} \quad \text{and} \quad \beta_2 = \begin{cases} \beta_{20}, & t \le T_{on}, \\ \beta_{2c}, & T_{on} < t \le T_{off}, \\ \beta_{20}, & t > T_{off}, \end{cases}$$

where

$$\beta_{10} = \frac{\beta c_0 + c_0 q_0(1-\beta)}{N},\ \beta_{20} = \frac{\beta c_0(1-q_0)}{N},\ \beta_{1c} = \frac{\beta c_c + c_c q_c(1-\beta)}{N} \text{ and } \beta_{2c} = \frac{\beta c_c(1-q_c)}{N}.$$

Moreover, $\beta_{10} > \beta_{20}$, $\beta_{1c} > \beta_{2c}$ and $\beta_{20} \ge \beta_{2c}$. Correspondingly, the model has three basic reproduction numbers $R_{01} = \frac{\beta_{20}S_0}{\gamma}$, $R_{02} = \frac{\beta_{2c}S(T_{on})}{\gamma}$ and $R_{03} = \frac{\beta_{20}S(T_{off})}{\gamma}$, and two effective reproduction numbers $R_{e1} = \frac{\beta_{20}S(t)}{\gamma}$, $t \in [0, T_{on}] \cup [T_{off}, +\infty)$ and $R_{e2} = \frac{\beta_{2c}S(t)}{\gamma}$, $t \in [T_{on}, T_{off}]$. Solving the above equation (4.1) in the interval $[0, T_{on}]$ with initial value (S_0, I_0), we obtain

$$I(t) + \frac{\beta_{20}}{\beta_{10}}S(t) - \rho_{10}\ln(S(t)) = \phi_{10},\ t \in [0, T_{on}], \tag{4.2}$$

where

$$\rho_{10} \doteq \frac{\gamma}{\beta_{10}} \text{ and } \phi_{10} \doteq I_0 + \frac{\beta_{20}}{\beta_{10}}S_0 - \rho_{10}\ln(S_0).$$

For convenience, we let $I_{T_{on}} \doteq I(T_{on})$ and $S_{T_{on}} \doteq S(T_{on})$, then

$$I_{T_{on}} = -\frac{\beta_{20}}{\beta_{10}}S_{T_{on}} + \rho_{10}\ln(S_{T_{on}}) + \phi_{10}.$$

Similarly, solving equation (4.1) in the interval $[T_{on}, T_{off}]$ with initial value $(S_{T_{on}}, I_{T_{on}})$, we obtain

$$I(t) + \frac{\beta_{2c}}{\beta_{1c}}S(t) - \rho_{1c}\ln(S(t)) = \phi_{1c},\ t \in (T_{on}, T_{off}], \tag{4.3}$$

where

$$\rho_{1c} \doteq \frac{\gamma}{\beta_{1c}} \text{ and } \phi_{1c} \doteq \left(\frac{\beta_{2c}}{\beta_{1c}} - \frac{\beta_{20}}{\beta_{10}}\right) S_{T_{on}} - (\rho_{1c} - \rho_{10}) \ln(S_{T_{on}}) + \phi_{10}.$$

Let $I_{T_{off}} \doteq I(T_{off})$ and $S_{T_{off}} \doteq S(T_{off})$, then

$$I_{T_{off}} = -\frac{\beta_{2c}}{\beta_{1c}} S_{T_{off}} + \rho_{1c} \ln\left(\frac{S_{T_{off}}}{S_{T_{on}}}\right) + \left(\frac{\beta_{2c}}{\beta_{1c}} - \frac{\beta_{20}}{\beta_{10}}\right) S_{T_{on}} + \rho_{10} \ln(S_{T_{on}}) + \phi_{10}.$$

Further, solving equation (4.1) for $t > T_{off}$ with initial value $(S_{T_{off}}, I_{T_{off}})$, we obtain

$$I(t) + \frac{\beta_{20}}{\beta_{10}} S(t) - \rho_{10} \ln(S(t)) = \phi_{12}, \ t \in (T_{off}, +\infty), \tag{4.4}$$

where

$$\phi_{12} \doteq \left(\frac{\beta_{20}}{\beta_{10}} - \frac{\beta_{2c}}{\beta_{1c}}\right)(S_{T_{off}} - S_{T_{on}}) + (\rho_{1c} - \rho_{10}) \ln\left(\frac{S_{T_{off}}}{S_{T_{on}}}\right) + \phi_{10}.$$

4.1. The maximum number of non-isolated infected individuals

Before the description of our results, let us now introduce the following Lemmas that will be used in this work.

Lemma 4.1. *For system (4.1), there is a unique peak of the number of non-isolated infected individuals if and only if the parameters T_{on} and T_{off} satisfy one of the following properties:*

(a_1) $R_{e1}(T_{on}) > 1$, $R_{02} > 1$, $R_{e2}(T_{off}) \geq 1$ *and* $R_{03} > 1$;

(a_2) $R_{e1}(T_{on}) > 1$, $R_{02} > 1$, $R_{e2}(T_{off}) < 1$ *and* $R_{03} \leq 1$;

(a_3) $R_{e1}(T_{on}) > 1$, $R_{02} > 1$, $R_{e2}(T_{off}) \geq 1$ *and* $R_{03} \leq 1$;

(a_4) $R_{e1}(T_{on}) > 1$, $R_{02} \leq 1$, $R_{e2}(T_{off}) < 1$ *and* $R_{03} \leq 1$.

Proof. From the second equation of system (4.1) and the property of $I(t)$, it is easy to verify the above conclusions, we omit the procedures for brevity. □

Lemma 4.2. *For system (4.1), there are two peaks of the number of non-isolated infected individuals if and only if the parameters T_{on} and T_{off} satisfy one of the following properties:*

(a_5) $R_{e1}(T_{on}) > 1$, $R_{02} > 1$, $R_{e2}(T_{off}) < 1$ *and* $R_{03} > 1$;

(a_6) $R_{e1}(T_{on}) > 1$, $R_{02} \leq 1$, $R_{e2}(T_{off}) < 1$ *and* $R_{03} > 1$.

Proof. It is easy to verify the above conclusions and we omit the procedures for brevity, which will be illustrated as follows. □

For cases (a_1)-(a_4) in Lemma 4.1, it is easy to verify that the peak of the number of non-isolated infected individuals could appear in the following four cases: after the second intervention, during the second intervention, at the start of the second intervention, and at the end of the second intervention, respectively. Let T_p^c be the time at which the number of non-isolated infected individuals reaches the peak, then T_p^c satisfies $T_p^c > T_{off}$, $T_{on} < T_p^c < T_{off}$, $T_p^c = T_{on}$ and $T_p^c = T_{off}$ for the above four cases (a_1)-(a_4), respectively. For cases (a_5) and (a_6), the first peak of the number of non-isolated infected individuals may appear at the start of the second intervention or during the second intervention. The second peak of the number of non-isolated infected individuals appears after the second intervention. The peak with a larger number gives the global maximum since there are two peaks of the numbers of non-isolated infected individuals.

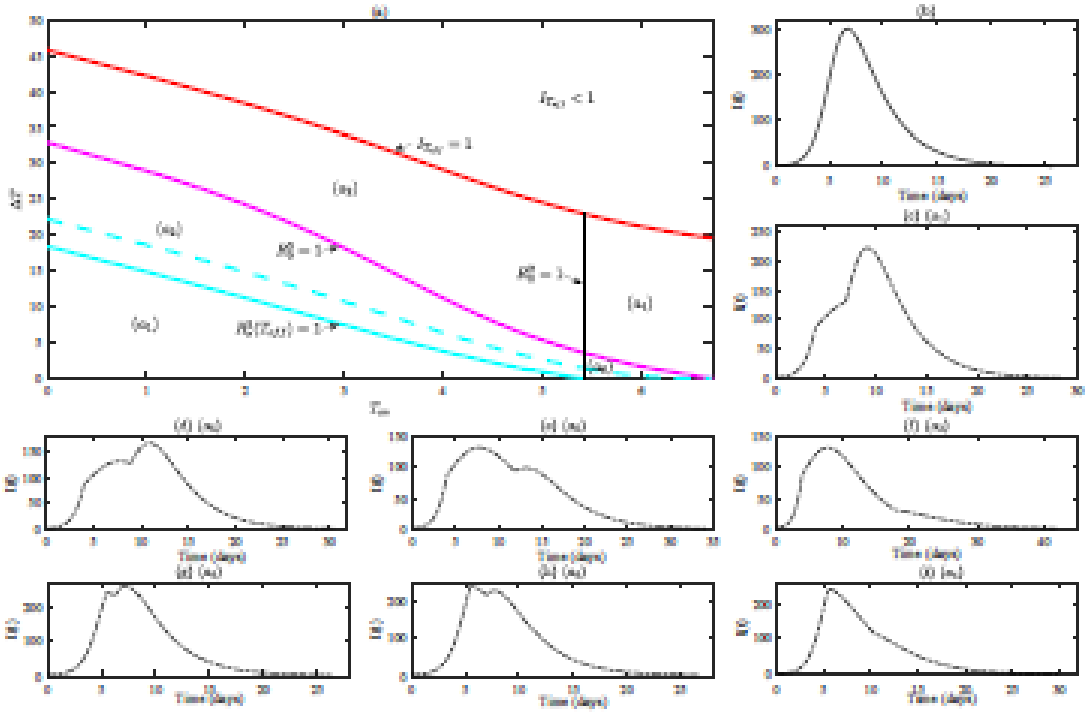

Figure 3: Impact of the timing of the second invention, where $\Delta T \doteq T_{off} - T_{on}$ represents the duration of the second intervention. (a) The distribution of the cases (a_1)-(a_5) and (a_1)-(a_5) in Lemmas 4.1 and 4.2 on the plane of $(T_{on}, \Delta T)$, and the cyan dashed curve represents that there exist two identical peaks of the number of non-isolated infected individuals. (b) The time-evolution of I for epidemics without a second intervention. (c)-(j) The time-evolution of I for epidemics with a second intervention, where (c) $(T_{on}, \Delta T) = (4, 3)$, (d) $(T_{on}, \Delta T) = (4, 5)$, (e) $(T_{on}, \Delta T) = (4, 8)$, (f) $(T_{on}, \Delta T) = (4, 14)$, (g) $(T_{on}, \Delta T) = (5.5, 0.8)$, (h) $(T_{on}, \Delta T) = (5.5, 1.5)$ and (i) $(T_{on}, \Delta T) = (5.5, 5)$. Other parameters are as follows: $N = 763$, $S_0 = 762$, $I_0 = 1$, $\beta = 0.155$, $c_0 = 10$, $q_0 = 0.01526$, $c_c = 4.58$, $q_c = 0.033$, $\gamma_I = 0.1$ and $\delta_I = 0.2504$.

To briefly illustrate the six cases in Lemmas 4.1 and 4.2, we fix $N = 763$, $S_0 = 762$, $I_0 = 1$, $\beta = 0.155$, $c_0 = 10$, $q_0 = 0.01526$, $c_c = 4.58$, $q_c = 0.033$, $\gamma_I = 0.1$ and $\delta_I = 0.2504$. In Fig.3 (a), we divide the $(T_{on}, \Delta T)$ parameter space into five subregions in which the cases (a_1)-(a_2) and (a_4)-(a_5) in Lemmas 4.1 and 4.2 are indicated, where $\Delta T \doteq T_{off} - T_{on}$ represents the duration of the second intervention. For case (a_3), the conditions $R_{e2}(T_{off}) \geq 1$ and $R_{02} \leq 1$ are equivalent to $\beta_{2c} = \beta_{20} = \frac{\gamma}{S_{T_{off}}}$, i.e. $\frac{\beta c_0(1-q_0)}{N} = \frac{\beta c_c(1-q_c)}{N}$, $c_0 = c_c$ and $q_0 = q_c$, which indicates that the intervention was not changed during the second intervention. Therefore, we omit it.

Remark 4.1. *In Lemmas 4.1 and 4.2, we theoretically analyze the number of the peaks for the number of non-isolated infected individuals. Note that (i) the peak of the number of non-isolated infected individuals may appear before the second intervention, i.e. the number of non-isolated infected individuals reaches its maximum before the second intervention. This case implies that the second intervention starts too late and fails to mitigate outbreaks. Therefore, we suppose that the second intervention should be implemented (or the intervention should be strengthened) before the peak of the number of non-isolated infected individuals. (ii) Here $R_{02} > 1$ implies that a weak intervention [17], i.e. the number of non-isolated infected individuals may increase during the second intervention period, as shown in Fig.3 (c)-(f). While $R_{02} < 1$ implies that a strong intervention [17], i.e. once the second intervention is implemented, the number of non-isolated infected individuals will decrease, as shown in Fig.3 (g)-(i). Furthermore, comparing the case (a_4) in Lemma 4.1 with the case (a_5) in Lemma 4.2, we can find that there is a second peak for the case (a_5), as shown in Fig.3 (g)-(h). This shows that the condition $R_{02} > 1$ is necessary for the existence of the second peak. This also implies that herd immunity is not achieved during the second intervention.*

Now let us describe the cases (a_1)-(a_2) and (a_4)-(a_6) in Lemmas 4.1 and 4.2 with respect to the maximum number of non-isolated infected individuals in detail. For convenience, let I^c_{max} and T^c_{max} be the maximum number of non-isolated infected individuals and the time at which the number of non-isolated infected individuals reaches the maximum in system (4.1), respectively. By a simple calculation, we have the following results.

Theorem 4.1. *For system (4.1), the maximum number of non-isolated infected individuals is given as*

$$I^c_{max} = \begin{cases} I_1, & for\ case(a_1), \\ I_2, & for\ case(a_2), \\ I_{T_{on}}, & for\ case(a_4), \\ max\{I_1, I_2\}, & for\ case(a_5), \\ max\{I_{T_{on}}, I_1\}, & for\ case(a_6), \end{cases}$$

where

$$I_1 = -\frac{\gamma}{\beta_{10}} + \rho_{10}\ln\left(\frac{\gamma}{\beta_{20}}\right) + \left(\frac{\beta_{20}}{\beta_{10}} - \frac{\beta_{2c}}{\beta_{1c}}\right)(S_{T_{off}} - S_{T_{on}}) + (\rho_{1c} - \rho_{10})\ln\left(\frac{S_{T_{off}}}{S_{T_{on}}}\right) + \phi_{10},$$

and

$$I_2 = -\frac{\gamma}{\beta_{1c}} + \rho_{1c}\ln\left(\frac{\gamma}{\beta_{2c}}\right) + \left(\frac{\beta_{2c}}{\beta_{1c}} - \frac{\beta_{20}}{\beta_{10}}\right)S_{T_{on}} - (\rho_{1c} - \rho_{10})\ln(S_{T_{on}}) + \phi_{10}.$$

Proof. For case (a_1) in Lemma 4.1, the number of non-isolated infected individuals reaches its maximum after the second intervention i.e. $T^c_{max} > T_{off}$. The conditions for the peaks are given in terms of the number of susceptible individuals as $S(t) = \frac{\gamma}{\beta_{20}}$ without the second intervention, and $S(t) = \frac{\gamma}{\beta_{2c}}$ with the second intervention. Correspondingly, we have $S_{T^c_{max}} = \frac{\gamma}{\beta_{20}}$. From equation (4.3), we have

$$I(t) + \frac{\beta_{20}}{\beta_{10}}S(t) - \rho_{10}\ln(S(t)) = \phi_{12},\ \ t \in [T_{off}, +\infty). \tag{4.5}$$

Substituting $S_{T^c_{max}} = \frac{\gamma}{\beta_{20}}$ into the above equation at time $t = T^c_{max}$, we obtain

$$I_{T^c_{max}} + \frac{\gamma}{\beta_{10}} - \rho_{10}\ln\left(\frac{\gamma}{\beta_{20}}\right) = \phi_{12},$$

i.e. the maximum number of non-isolated infected individuals is

$$I_{T^c_{max}} = -\frac{\gamma}{\beta_{10}} + \rho_{10}\ln\left(\frac{\gamma}{\beta_{20}}\right) + \left(\frac{\beta_{20}}{\beta_{10}} - \frac{\beta_{2c}}{\beta_{1c}}\right)(S_{T_{off}} - S_{T_{on}}) + (\rho_{1c} - \rho_{10})\ln\left(\frac{S_{T_{off}}}{S_{T_{on}}}\right) + \phi_{10}, \tag{4.6}$$

which is equivalent to I_1 giving the maximum number of non-isolated infected individuals for case (a_1). The others can be proved similarly, and we omit the procedures for brevity. The proof is completed. □

Remark 4.2. *For system (4.1), there are two identical peaks of the number of non-isolated infected individuals when $I_1 = I_2$ for case (a_3). Similarly, there also exist two identical peaks of the number of non-isolated infected individuals when $I_{T_{on}} = I_1$ for case (a_6), as shown in Fig 3 (a).*

In Theorem 4.1, we summarize the analytical forms of the maximum number of non-isolated infected individuals for cases (a_1)-(a_2) and (a_4)-(a_6) with respect to the number of susceptible individuals at the start and end of the second intervention, $S_{T_{on}}$ and $S_{T_{off}}$. We cannot directly analyse the impact of the timing of the second intervention on the maximum number of non-isolated infected individuals since it is difficult to obtain the time series of the system (4.1) analytically without any approximations. Note that there exists a one-to-one correspondence between (T_{on}, T_{off}) and $(S_{T_{on}}, S_{T_{off}})$. It follows from the first equation of system (4.1) that $S_{T_{on}}$ and $S_{T_{off}}$ are monotonically

decreasing with respect to T_{on} and T_{off}, respectively, i.e. $\frac{\partial S_{I_{max}}}{\partial T_{on}} < 0$ and $\frac{\partial S_{T_{off}}}{\partial T_{off}} < 0$. Therefore, we can analyse the impact of the timing of the second intervention on the maximum number of non-isolated infected individuals by using this method. See Appendix A for details of the derivation.

4.2. The time needed to realize the dynamic zero-case

Let T^c_{end} ($T^c_{end} \geq T_{off}$) be the time needed to realize the dynamic zero-case aim in system (4.1). Correspondingly, we have the following results.

Theorem 4.2. *For system (4.1), the time needed to realize the dynamic zero-case aim is given as*

$$T^c_{end} = T_{off} + \int_{S_{T_{off}}}^{S_{T^c_{end}}} \frac{1}{S[\beta_{20}S - \beta_{10}\rho_{10}\ln(S) - \beta_{10}\phi_{12}]} dS,$$

where

$$S_{T^c_{end}} \doteq -\frac{\beta_{10}\rho_{10}}{\beta_{20}} Lambert\ W\left[0, -\frac{\beta_{20}}{\beta_{10}\rho_{10}} exp\left(\frac{1-\phi_{12}}{\rho_{10}}\right)\right] < \frac{\gamma}{\beta_{20}}.$$

Proof. For equation (4.3), we have

$$I(t) = -\frac{\beta_{20}}{\beta_{10}} S(t) + \rho_{10}\ln(S(t)) + \phi_{12},\ t \in [T_{off}, +\infty), \tag{4.7}$$

and it follows from $I_{T^c_{end}} = 1$ and $I'(T^c_{end}) < 0$ at time $t = T^c_{end}$ that

$$1 + \frac{\beta_{20}}{\beta_{10}} S_{T^c_{end}} - \rho_{10}\ln(S_{T^c_{end}}) = \phi_{12} \tag{4.8}$$

and $S_{T^c_{end}} < \frac{\gamma}{\beta_{20}}$. By using the Lambert W function [29], solving equation (4.8) with respect to $S_{T^c_{end}}$, we obtain

$$S_{T^c_{end}} = -\frac{\beta_{10}\rho_{10}}{\beta_{20}} Lambert\ W\left[0, -\frac{\beta_{20}}{\beta_{10}\rho_{10}} exp\left(\frac{1-\phi_{12}}{\rho_{10}}\right)\right].$$

Substituting equation (4.7) into the first equation of system (4.1) yields

$$S'(t) = S[\beta_{20}S - \beta_{10}\rho_{10}\ln(S) - \beta_{10}\phi_{12}],\ t \in [T_{off}, +\infty). \tag{4.9}$$

Further, we integrate equation (4.9) from time T_{off} to T^c_{end}:

$$\int_{S_{T_{off}}}^{S_{T^c_{end}}} \frac{1}{S[\beta_{20}S - \beta_{10}\rho_{10}\ln(S) - \beta_{10}\phi_{12}]} dS = \int_{T_{off}}^{T^c_{end}} dt.$$

Then, the time needed to realize the dynamic zero-case aim is

$$T^c_{end} = T_{off} + \int_{S_{T_{off}}}^{S_{T^c_{end}}} \frac{1}{S[\beta_{20}S - \beta_{10}\rho_{10}\ln(S) - \beta_{10}\phi_{12}]} dS.$$

This completes the proof. □

Remark 4.3. *For system (4.1), note that at time $t = T_{off}$, $I_{T_{off}} \geq 1$, which is equivalent to*

$$T_{off} \leq T_{on} + \int_{S_{T_{on}}}^{-\frac{\beta_{1c}\rho_{1c}}{\beta_{2c}} Lambert\ W\left[0, -\frac{\beta_{2c}}{\beta_{1c}\rho_{1c}} exp\left(\frac{1-\phi_{1c}}{\rho_{1c}}\right)\right]} \frac{1}{S[\beta_{2c}S - \beta_{1c}\rho_{1c}\ln(S) - \beta_{1c}\phi_{1c}]} dS \doteq T^{max}_{off}.$$

Otherwise, when $T_{off} > T_{off}^{max}$, then we have $I_{T_{off}} < 1$, which indicates that the second intervention will not be stopped until the infectious disease is eradicated outside quarantined areas, i.e. realizing the dynamic zero-case policy.

5. Numerical investigations and results

In the previous section, we obtained the maximum number of non-isolated infected individuals (I_{max}^c) and the time (T_{end}^c) needed to realize the dynamic zero-case aim for all cases in Lemmas 4.1 and 4.2 by theoretical analysis. It shows that I_{max}^c depends on the number of susceptible individuals at the start and end of the second intervention, $S_{T_{on}}$ and $S_{T_{off}}$, and T_{end}^c depends on T_{off}, $S_{T_{on}}$ and $S_{T_{off}}$. However, although there exists a one-to-one correspondence between (T_{on}, T_{off}) and $(S_{T_{on}}, S_{T_{off}})$, it is difficult to analyse the impact of the timing of the second intervention on the maximum number of non-isolated infected individuals and the time needed to realize the dynamic zero-case aim, which will be further addressed in the coming sections by numerical investigations. Furthermore, we introduce close contact tracing into the classical SIR model. To better understand the role of control measures on the maximum number of non-isolated infected individuals and the time needed to realize the dynamic zero-case aim, we carry out the numerical analyses with respect to the two key parameters q_c and c_c, which allow us to compare the main results with those obtained for the classical SIR model with one-shot intervention [15–17].

5.1. Impact of the timing of the second intervention (T_{on} and T_{off})

Based on the methods proposed in [17], we address the impact of the timing of the second intervention on the maximum number of non-isolated infected individuals and the time needed to realize the dynamic zero-case aim under strong intervention ($R_{02} < 1$) and weak intervention ($R_{02} > 1$),respectively.

5.1.1. The strong second intervention ($R_{02} < 1$)

Here I_{max}^c and T_{end}^c are numerically calculated with different start and end times for the second intervention, T_{on} and T_{off} ($T_{off} = T_{on} + \Delta T$). To better illustrate the impact of the second intervention, I_{max}^c is normalized in the absence of the second intervention by I_{max}^{no}, and T_{end}^c is normalized in the absence of the second intervention by T_{end}^{no}. I_{max}^c/I_{max}^{no} and T_{end}^c/T_{end}^{no} quantify the effectiveness of the second intervention. As I_{max}^c/I_{max}^{no} decreases, the second intervention shows more success in minimizing the maximum number of non-isolated infected individuals. Similarly, as T_{end}^c/T_{end}^{no} decreases, the second intervention shows more success in shortening the time needed to realize the dynamic zero-case aim.

In Fig.4, we let $N = 763$, $S_0 = 762$, $I_0 = 1$, $\beta = 0.155$, $c_0 = 10$, $q_0 = 0.01526$, $c_c = 2.5$, $q_c = 0.21$, $\gamma = 0.1$ and $\delta_I = 0.2504$. Once the second intervention is implemented (or the intervention is strengthened), the number of non-isolated infected individuals will decrease. There are one and two peaks in the regions (a_4) and (a_5), respectively. The maximum number of non-isolated infected individuals is smaller than that without the second intervention, appearing at the start of the second intervention and after the second intervention. More precisely, it appears at the start of the second intervention in the region to the right of the cyan dashed curve, after the second intervention in the region to the left of the cyan dashed curve, as shown in Fig.4 (a). The dependence of the time needed to realize the dynamic zero-case aim on the timing of the second intervention is plotted in Fig.4 (b). Note that there exists a one-to-one correspondence between Fig.4 (a) and (b).

- More individuals may be infected at the peak of the second wave with a stronger intervention during the epidemic. As shown in Fig.4 (e), once the second intervention is implemented, the number of non-isolated infected individuals will decrease. However, there is a larger second peak after the second intervention even if the second intervention is longer. This would effectively discard the efforts that had been made during the second intervention, provoking a critical failure of the health care system. Therefore, it will be necessary to be alert for a larger second wave that may occur after the second intervention in such cases.

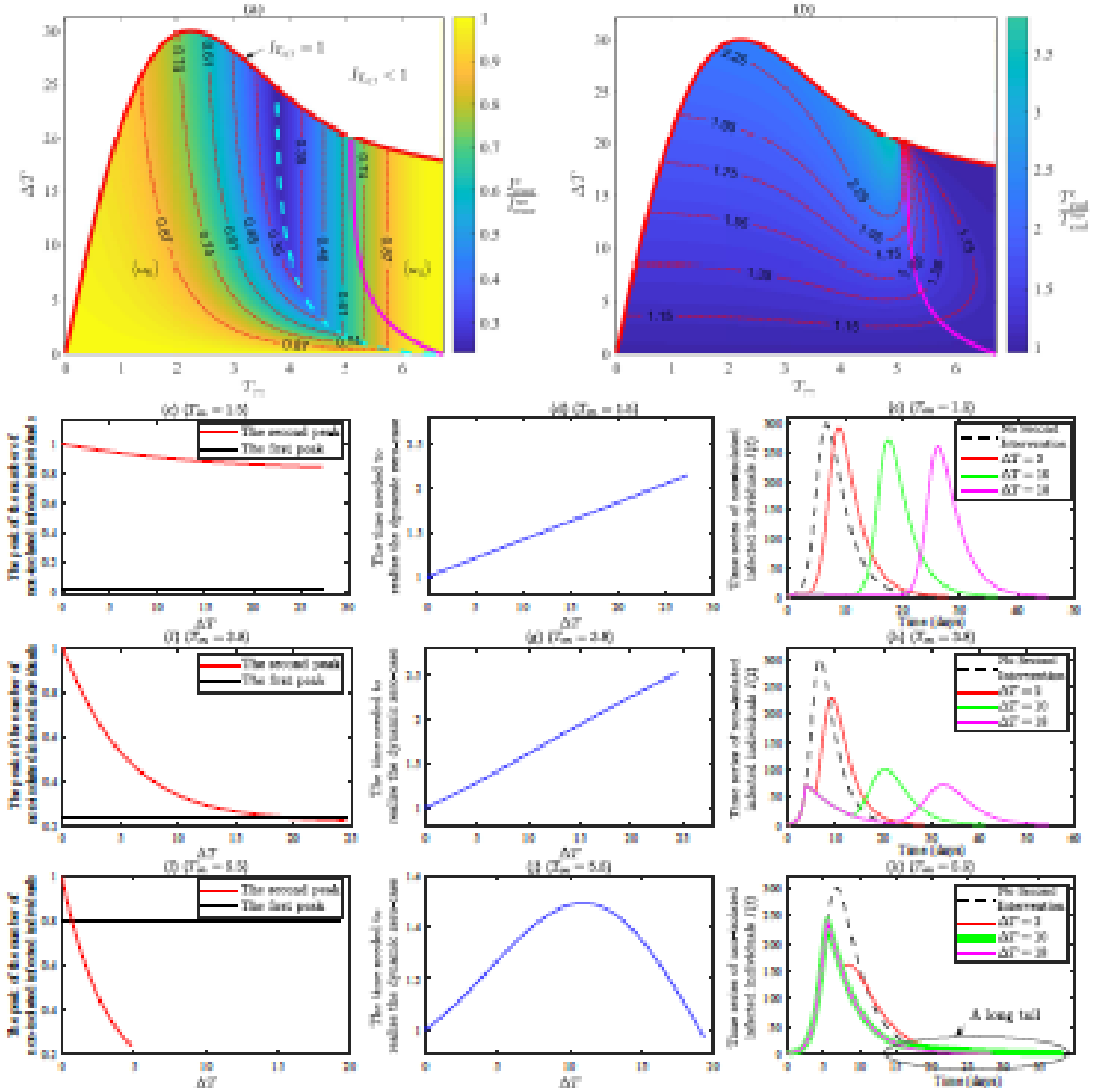

Figure 4: Impact of the timing of the strong second intervention ($R_{02} < 1$) on the maximum number of non-isolated infected individuals and the time needed to realize the dynamic zero-case aim. Here we fix all other parameters as follows: $N = 763$, $S_0 = 762$, $I_0 = 1$, $\beta = 0.155$, $\alpha_1 = 10$, $q_0 = 0.01526$, $c_r = 2.5$, $q_r = 0.21$, $\gamma_I = 0.1$ and $\delta_I = 0.2504$. (a) The maximum number of non-isolated infected individuals (I^*_{max}) with respect to T_{on} and ΔT, where the cyan dashed curve represents that there exist two identical peaks of the number of non-isolated infected individuals, the purple solid curve is the boundary of regions (a_1) and (a_2). (b) The time (T^*_{dyn}) needed to realize the dynamic zero-case aim with respect to T_{on} and ΔT. (c), (f) and (i) represent the peak of the number of non-isolated infected individuals. (d), (g) and (j) represent the times needed to realize the dynamic zero-case aim. (e), (h) and (k) Time series of the number of non-isolated infected individuals.

- As shown in Fig.4 (a) and (h), the maximum number of non-isolated infected individuals is minimized in the intermediate start of the second intervention T_{on}, when the peaks at the start of the second intervention and after the second intervention are identical. This implies that early implementation of the second intervention does not necessarily minimize the number of non-isolated infected individuals. Intuitively, early initiation of the second intervention has largely curbed the spread of the disease. However, the early onset of the second

intervention also protects a large number of susceptible individuals, which could result in a large second wave after the second intervention. Thus, the early second intervention may be not effective, as shown in Fig.4 (e).

- I^c_{max}/I^{nc}_{max} is always less than unity and T^c_{end}/T^{nc}_{end} is always larger than unity in the presence of the second intervention, as shown in Fig.4 (a) and (b). This means that implementing the second intervention does not shorten the time that it takes to realize the dynamic zero-case aim. In particular, if the maximum number of non-isolated infected individuals occurs in the region (a_s), T^c_{end} is monotonically increasing which depends on ΔT for any fixed T_{on}, as shown in Fig.4 (b), (d) and (g). This implies that extending the duration of the second intervention may prolong the time that it takes to realize the dynamic zero-case policy even if the second intervention starts early. Note that it takes longer to realize the dynamic zero-case policy due to there being a second wave caused by the strong intervention.

- If the maximum number of non-isolated infected individuals occurs in the region (a_s), T^c_{end} is an upward convex function of ΔT, as shown in Fig.4 (j). In this case, there is no second wave, and the maximum number of non-isolated infected individuals only depends on T_{on}. This implies that, in this case, extending the duration of the second intervention not only does not reduce the maximum number of non-isolated infected individuals but it also may prolong the time needed to realize the dynamic zero-case aim. It is worth mentioning that (*i*) there is a critical value ΔT^* which satisfies $(T^c_{end})'(\Delta T^*) = 0$. When $\Delta T > \Delta T^*$, T^c_{end} decreases as ΔT continues to increase. This means that only if the second intervention lasts long enough, it may be effective in shortening the time needed to realize the dynamic zero-case. (*ii*) It is clear that there is a "long tail" of $I(t)$, as shown in Fig.4 (k). In this case, the number of non-isolated infected individuals declines slowly, and it takes longer to realize the dynamic zero-case policy even if there are few non-isolated infected individuals after the second intervention.

5.1.2. The weak second intervention ($R_{02} > 1$)

In Fig.5, we let $c_c = 4.58$ and $q_c = 0.033$, and fix all other parameter values as those in Fig.4. In this situation, the number of non-isolated infected individuals will continue to increase after the start of the second intervention. Therefore, the maximum number of non-isolated infected individuals appears during the second intervention or after it, as shown in Fig.5 (e) and (h). It follows from Fig.5 (a) that I^c_{max} is quasi-monotonically decreasing with respect to ΔT for any fixed T_{on}, i.e., as ΔT increases, I^c_{max} will decrease and then be maintained. This implies that a longer second intervention duration does not reduce the maximum number of non-isolated infected individuals. Thus, for the purpose of reducing the maximum number of the non-isolated infected individuals and shortening the duration of the second intervention (ΔT), the optimal time to end the second intervention is when they can control the peak value of a second rebound of the epidemic to be equal to the first peak value. Furthermore, the earlier the second interventions, the more effective they are and the smaller the maximum number of non-isolated infected individuals.

In terms of the time needed to realize the dynamic zero-case aim, it is clear that T^c_{end}/T^{nc}_{end} is also larger than unity in the presence of the second intervention, as shown in Fig.5 (b). The difference from Fig.4 (b) is that T^c_{end} is an upward convex function of ΔT for any fixed T_{on} in Fig.5 (b), which implies that regardless of whether the second intervention starts earlier or later, only if the second intervention lasts long enough, it may be effective in shortening the time needed to realize the dynamic zero-case. Similarly, there is also a "long tail" of $I(t)$, as shown in Fig.5 (e) and (h).

5.2. Impact of two control measures q_c and c_c

To better reveal the impact of the two control measures q_c and c_c on the maximum number of non-isolated infected individuals (I^c_{max}) and the time (T^c_{end}) needed to realize the dynamic zero-case aim, we denote $\Delta q = q_c - q_0$ and $\Delta c = c_0 - c_c$ with $q_c > q_0$ and $c_c < c_0$. This indicates that the bigger the value of Δq, the stronger the close contact tracing during the second intervention and the bigger the value of Δc, the fewer the number of contacts per infected individual. The main results are shown in Figs.6 and 7.

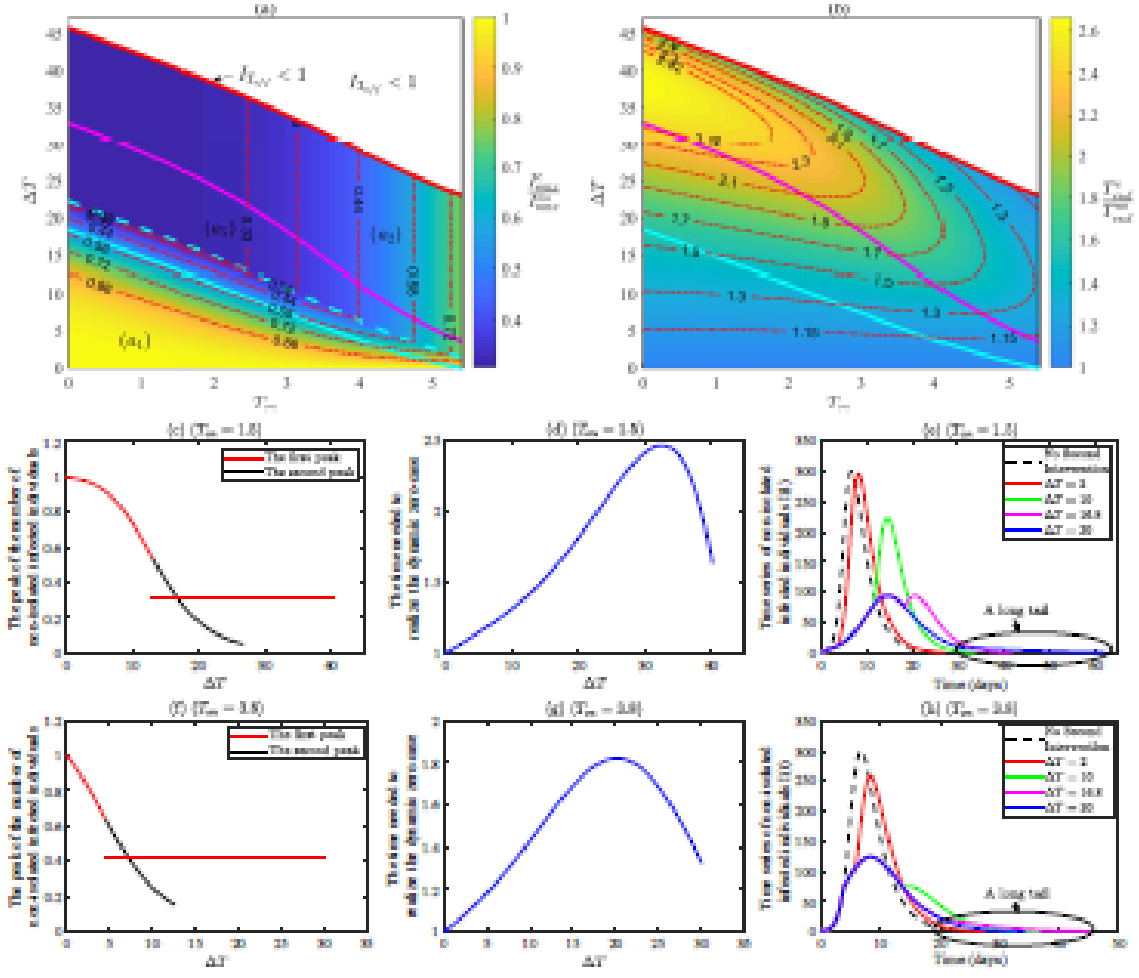

Figure 5: Impact of the timing of the weaker second intervention ($R_{02} > 1$) on the maximum number of non-isolated infected individuals and the time needed to realize the dynamic zero-case aim. Here we fix all other parameters as follows: $N = 763$, $S_0 = 762$, $I_0 = 1$, $\beta = 0.155$, $\sigma_I = 10$, $q_0 = 0.015\,26$, $\alpha_c = 4.58$, $q_c = 0.033$, $\gamma_I = 0.1$ and $\delta_I = 0.2904$. (a) The maximum number of non-isolated infected individuals (I^c_{max}) with respect to T_{in} and ΔT, where the purple and cyan solid curves divide the $(T_{in}, \Delta T)$ parameter space into three subregions corresponding to cases (a_1), (a_2) and (a_3) in Lemmas 4.1 and 4.2. The cyan dashed curve represents that there exist two identical peaks of the number of non-isolated infected individuals. (b) The time (T^c_{end}) needed to realize the dynamic zero-case aim with respect to T_{in} and ΔT. (c) and (f) represent the peak of the number of non-isolated infected individuals. (d) and (g) represent the times needed to realize the dynamic zero-case aim. (e) and (h) Time series of the number of non-isolated infected individuals.

In Fig.6, we consider the impact of the two control measures separately. As shown in Fig.6 (a), it is clear that for small ΔT, I^c_{max} is almost independent of Δq, which implies that the contact tracing strategy cannot make much difference in a shorter second intervention. For intermediate ΔT, I^c_{max} is quasi-monotonically decreasing with respect to Δq, i.e. as ΔT increases, I^c_{max} will decrease until $R_{02} = 1$ and then be maintained. When ΔT is large enough, I^c_{max} is monotonically decreasing with respect to Δq. Therefore, for a longer second intervention duration, a higher quarantine rate is optimal to minimize the maximum number of non-isolated infected individuals. In terms of the time needed to realize the dynamic zero-case aim, as shown in Fig.6 (b), we find that T^c_{end} is complicated as Δq varies for fixed ΔT. This shows that only when ΔT ($\Delta T > 12.23$ days) is large enough, T^c_{end} is monotonically decreasing with respect to Δq. In this case, T^c_{end}/T^{nc}_{end} is less than unity. Therefore, as suggested in Fig.6 (a) and (b), while extending the duration of the second intervention, it is also necessary to strengthen the intensity of contact

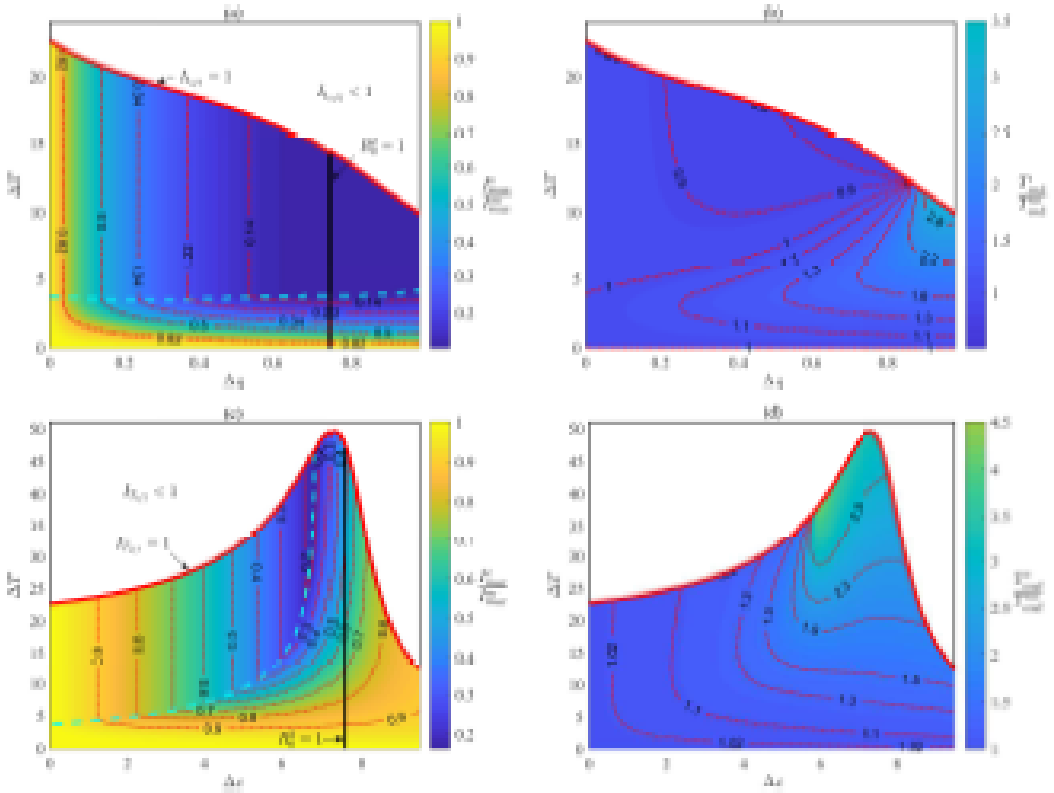

Figure 6 Impact of two control measures (q_c and c_c) on the maximum number of non-isolated infected individuals and the time needed to realize the dynamic zero-case aim, respectively. (a) and (b) The impact of increasing contact tracing rate (or isolated rate) with fixed contact rate ($c_c = c_3 = 10$). (c) and (d) The impact of reducing contact rate with fixed contact tracing rate ($q_c = q_3 = 0.01526$). The cyan dashed curve represents that there exist two identical peaks of the number of non-isolated infected individuals. Other parameters as follows: $N = 763$, $S_0 = 762, I_0 = 1$, $\beta = 0.155$, $q_0 = 0.01526$, $c_0 = 10$, $\gamma = 0.1$, $\delta_I = 0.2504$ and $T_{SI} = 3$.

tracing. Especially, when the duration of the second intervention is long enough, the stronger the contact tracing intensity, the more effective it is to minimize the maximum number of non-isolated infected individuals and shorten the time that it takes to realize the dynamic zero-case aim.

From Fig.6 (c), it is also shown that reducing the contact rate has little impact on the related indices in a shorter second intervention. The maximum number of the non-isolated infected individuals is minimized in the intermediate contact rate (c_c) and longer second intervention duration (ΔT), which implies that it not necessary to reduce the contact rate sufficiently. Compared with the results in Fig.6 (a), it is worth mentioning that the contact rate needs to be reduced to a very low level to get the same I^c_{max} as in Fig.6 (a). This implies that strengthening the contact tracing intensity is more effective than reducing the contact rate in minimizing the maximum number of infected individuals. That is, strengthening the contact tracing intensity can cut off the source of infection more effectively, but reducing the contact rate does not. As shown in Fig.6 (d), T^c_{end}/T^{no}_{end} is always larger than unity. The parameter space where the value of T^c_{end} is maximized is the parameter space where the value of I^c_{max} is minimized. This suggests that only reducing the contact rate can not shorten the time needed to realize the dynamical zero-case aim even if the duration of the second intervention is long enough.

In Fig.7, we fix the starts and ends of the secondary intervention to explore the impact of implementing the two control measures simultaneously. Fig.7 (a) and (c) show that the maximum number of the non-isolated infected individuals (I^c_{max}) is minimized in the intermediate or large contact rate (c_c) and large quarantine rate (q_c). This also implies that strengthening the contact tracing intensity is more important than reducing the contact rate in reducing the maximum number of non-isolated infected individuals, and reducing the contact rate sufficiently may

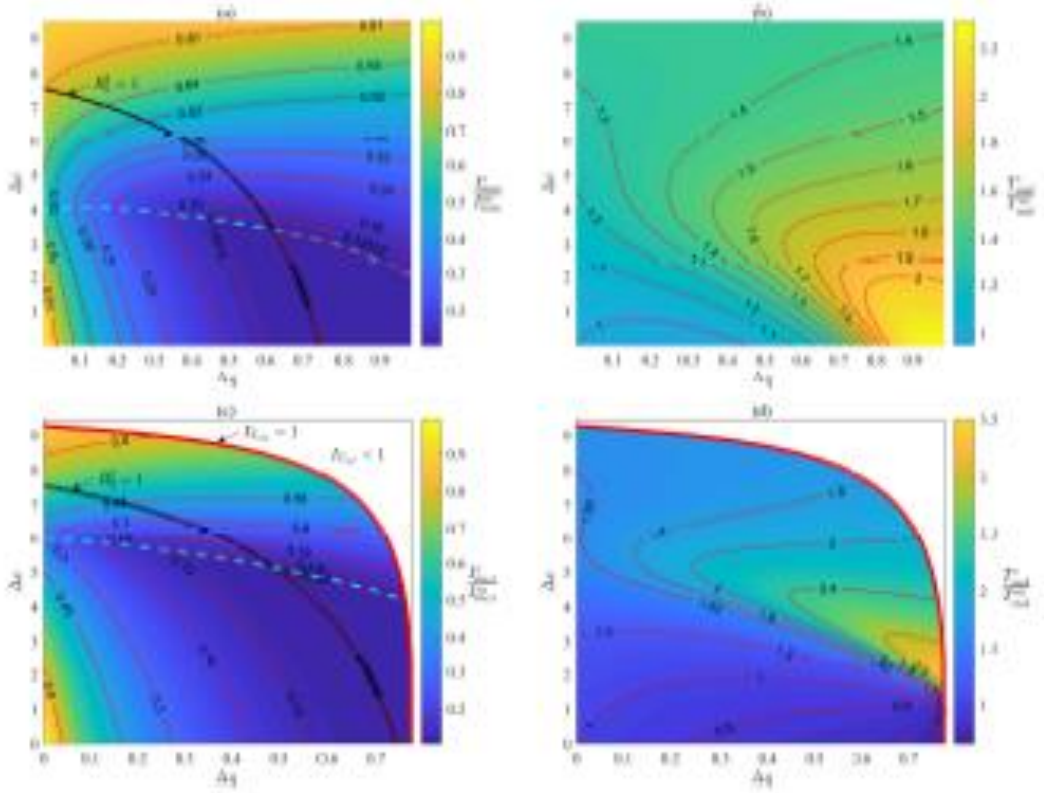

Figure 7. Impact of two control measures (q_c and c_c) simultaneously on the maximum number of non-isolated infected individuals and the time needed to realize the dynamic zero-case aim, with fixed starts (T_{on}) and ends (T_{off}) of the secondary intervention. (a) and (b) $T_{on} = 3$ and $T_{off} = 10$. (c) and (d) $T_{on} = 3$ and $T_{off} = 17$. The cyan dashed curve represents that there exist two identical peaks of the number of non-isolated infected individuals. Other parameters as follows: $N = 763$, $S_0 = 762$, $I_0 = 1$, $\beta = 0.155$, $q_0 = 0.01526$, $c_0 = 10$, $\gamma_I = 0.1$ and $\delta_I = 0.2504$.

be ineffective, which further verifies the results in Fig.6 (a) and (c). In terms of the time needed to realize the dynamic zero-case aim, compared with the results in Fig.7 (b) and (d), it is worth mentioning that with a longer intervention, an optimal parameter space of Δq and Δc can be found, where both I^c_{max} and T^c_{end} are minimized. This means that when the duration of the second intervention is not long enough, it may not shorten the time that it takes to realize the dynamic zero-case policy and achieve our goal of minimizing both I^c_{max} and T^c_{end} even if both control measures are implemented simultaneously.

6. The optimal intervention

Crucial and interesting questions are when and how to implement the second intervention such that both the maximum number of non-isolated infected individuals and the time needed to realize the dynamic zero-case aim are minimized. To do this, we define a multi-objective optimal control problem as follows:

$$\min_{T_{on},T_{off},c_c,q_c} \; G(T_{on},T_{off},c_c,q_c) \doteq [I^c_{max}(T_{on},T_{off},c_c,q_c), T^c_{end}(T_{on},T_{off},c_c,q_c)]^T, \tag{6.1}$$

s.t

$$\begin{cases} 0 < T_{on} < T_{on}^{max}, \; T_{on} < T_{off} < T_{off}^{max}, \\ q_0 \le q_c < 1, \; 0 < c_c \le c_0, \\ \text{equation (2.1) with (2.2).} \end{cases} \tag{6.2}$$

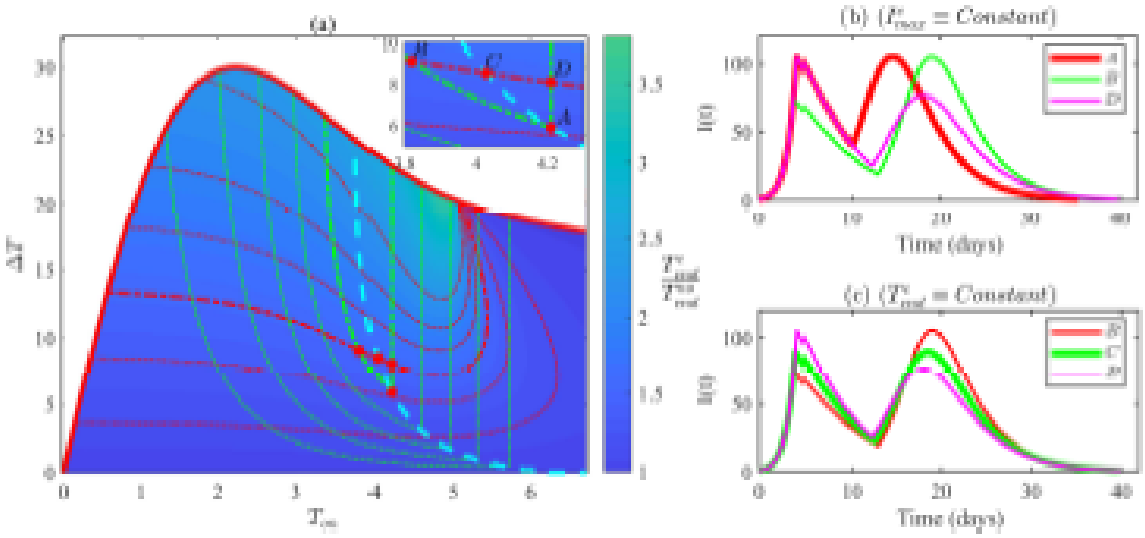

Figure 8: The optimal timing of the strong second intervention. (a) A combination of contour lines of Fig.4 (a) and (b), where the thick green dashed-dotted curve represents $I^c_{max} = 0.35I^{no}_{max}$, the thick red dashed-dotted curve represents $T^c_{end} = 1.55T^{no}_{end}$. (b) and (c) Time series of the number of non-isolated infected individuals, where A (4.21, 5.9), B(3.82, 9.1), C(4.028, 8.534) and D(4.21, 8.1).

It is difficult to find special parameter spaces for T_{on}, T_{off}, c_c and q_c such that both I^c_{max} and T^c_{end} are minimized because we cannot obtain the time series of system (2.1) with (2.2) analytically. For simplicity, we discuss the following two simple scenarios.

6.1. *Minimizing T^c_{end} with constant I^c_{max}*

Let I^c_{max} be a constant, i.e. choosing parameters T_{on}, T_{off}, c_c and q_c along a contour of I^c_{max}, and we discuss the following two scenarios:

- We assume that the contact rate c_c and quarantine rate q_c during the second intervention are constants, and T_{on} and T_{off} are varied. Minimizing the time (T^c_{end}) needed to realize the dynamic zero-case aim by choosing T_{on} and T_{off} along a contour of I^c_{max}. This case is studied in Fig.8. In Fig.8 (a), let $I^c_{max} = 0.35I^{no}_{max}$. Correspondingly, a contour crosses points B, A and D, as shown in Fig.8 (a). As we have discussed in the previous section, shorter second intervention durations are optimal to shorten the time needed to realize the dynamic zero-case aim. Namely, T^c_{end} is minimized near the point A, as shown in Fig.8 (a). Correspondingly, the time series of the number of non-isolated infected individuals at the point A is shown in Fig.8 (b). In this case, the optimal time to initiate the second intervention is when they can control the peak value of a second rebound of the epidemic to be equal to the first peak value.

- Assuming that T_{on} and T_{off} are constants, and c_c and q_c are varied. Minimizing the time (T^c_{end}) needed to realize the dynamic zero-case aim by choosing c_c and q_c along a contour of I^c_{max}. This case is studied in Fig.9. As shown in Fig.9 (a), let $I^c_{max} = 0.16I^{no}_{max}$, correspondingly, a contour crosses points A, B, C and D. In this case, along the contour of I^c_{max}, it is easy to obtain that T^c_{end} is minimized near the point D. The time series of the number of non-isolated infected individuals at the point D is shown in Fig.9 (b).

6.2. *Minimizing I^c_{max} with a constant T^c_{end}*

Another possible constraint is to minimize the maximum number of non-isolated infected individuals (I^c_{max}), keeping the time (T^c_{end}) constant, i.e. choosing parameters along the contour of T^c_{end}. In Fig.8, let the contact rate c_c and quarantine rate q_c during the second intervention be constants, and assume that T_{on} and T_{off} are varied, and we fix $T^c_{end} = 1.55T^{no}_{end}$ and mark the crossing points as B, C and D. Along the contour of T^c_{end} in Fig.8 (a), we find

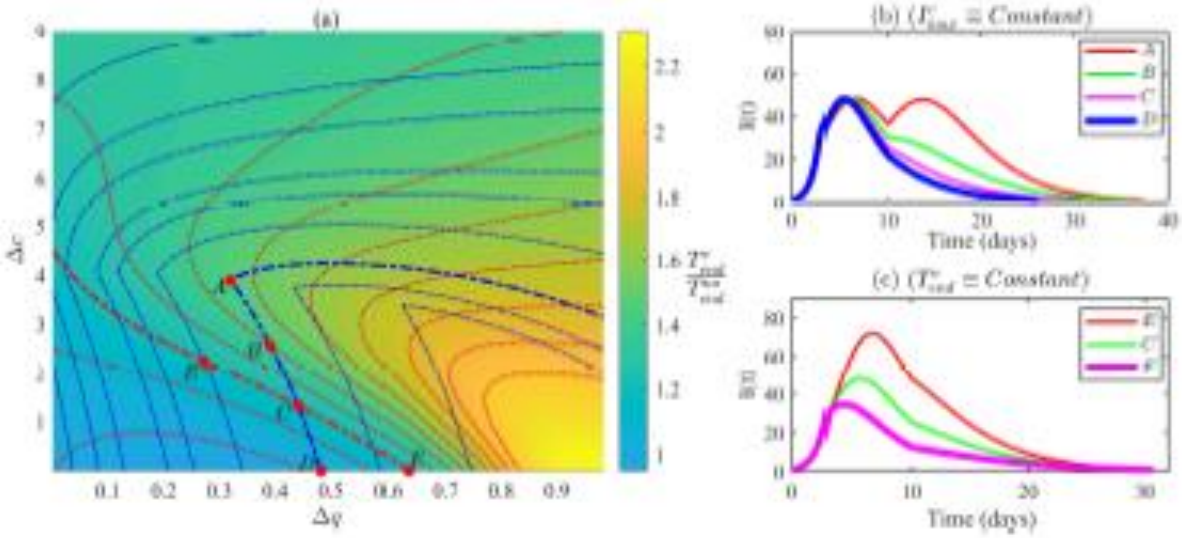

Figure 9: The optimal contact rate and quarantine rate with fixed timing of the second intervention. (a) A combination of contour lines of (a) and (b) in Fig.7. (b) and (c) Time series of the number of non-isolated infected individuals, where $A(0.272, 2.245)$, $B(0.441, 1.31)$, $C(0.634, 0)$, $D(0.319, 3.89)$, $E(0.391, 2.57)$ and $F(0.482, 0)$.

that I^c_{max} is minimized near the point C. The time series of the number of non-isolated infected individuals at the point C is shown in Fig.8 (c). The optimal parameter spaces for c_c and q_c can be determined by similar methods, as shown in Fig.9 (a) and (c).

7. Special case $T_{off} = T^c_{end}$

Under China's dynamic zero-case policy, once the prevention and control strategy is launched, it will last until the end of the epidemic, that is, until the dynamic zero-case goal is achieved. From the mathematical point of view, we have $T_{off} = T^c_{end}$ in system (4.1), and there exists a unique peak for non-quarantined infected individuals. It may appear at the start of the second intervention or during the second intervention. Correspondingly, we have the following results.

Theorem 7.1. *For system (4.1), when $T_{off} = T^c_{end}$, the maximum number of non-isolated infected individuals is given as*

$$I_{max} = \begin{cases} I_2, & R_{02} > 1, \\ I_{T_{on}}, & R_{02} \le 1. \end{cases}$$

The time needed to realize the dynamic zero-case aim is given as

$$T^c_{end} = T_{on} + \int_{S_{T_{on}}}^{-\frac{\beta_1 q_1 c_1}{\beta_{2c}} Lambert W\left[0, -\frac{\beta_{2c}}{\beta_1 q_1 c_1} exp\left(\frac{1-q_{1c}}{r_{1c}}\right)\right]} \frac{1}{S[\beta_{2c}S - \beta_1 q_1 c_1 \ln(S) - \beta_1 c_1 \phi_{1c}]} dS,$$

Proof. The proof is similar to those in Theorems 4.1 and 4.2, so we omit the procedures for brevity. □

For this case, to understand the effect of the timing of the second intervention and close contact tracing strategy on the maximum number of non-isolated infected individuals and the time needed to realize the dynamic zero-case aim, we also carry out the numerical analyses with the key parameters T_{on}, q_c and c_c, as shown in Appendix B. The results suggest that to minimize the maximum number of non-isolated infected individuals and shorten the time needed to realize the dynamic zero-case aim, the best strategy is to intervene early and fully strengthen the contact tracing intensity. See Appendix B for details.

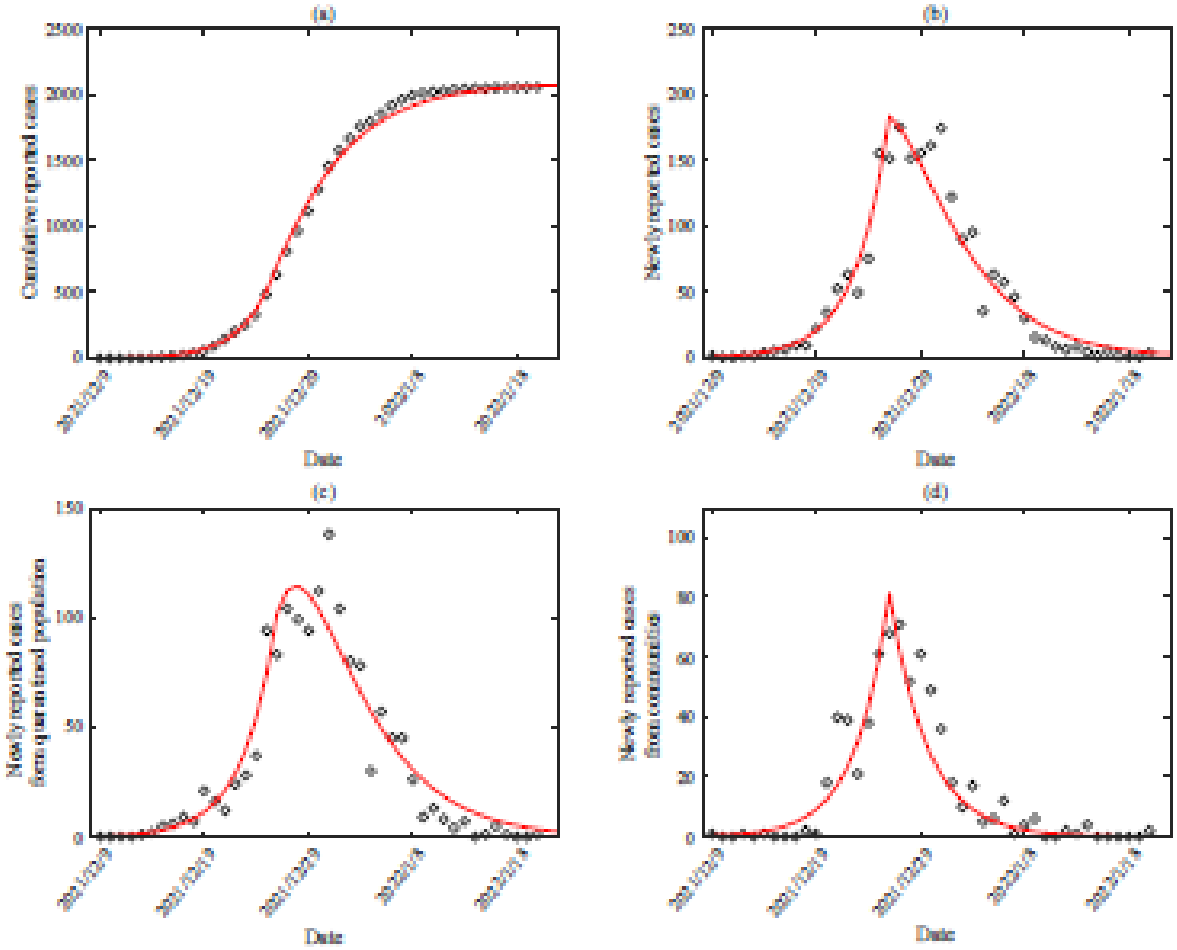

Figure 10: Fitting results of model (2.1) with (2.2) to the epidemic data in Xi'an from 9 December 2021 to 20 January 2022. (a) Fitting of cumulative number of reported cases; (b) Fitting of newly reported cases; (c) Fitting of newly reported cases from quarantined population; (d) Fitting of newly reported cases from communities. The black circles represent the reported data, the red curves are the simulation results.

8. Examination of data fitting for epidemics of COVID-19

The proposed model (2.1) with discontinuous contact and quarantine rates provide us with an effective switching strategy to mitigate and contain infectious diseases, which can be validated by the real data sets of various waves of COVID-19 epidemics in China. The newly reported cases from 9 December 2021 to 20 January 2022 in Xi'an were obtained from the Shaanxi Municipal Health Commission [30], which can be separated into the newly reported cases from the quarantined population, and the newly reported cases from communities (which are detected in untraced infected individuals). Data collected are shown in Fig.10, where the black circles represent the reported data.

To calibrate the model, we set the initial susceptible population as the total number of the population in Xi'an (Xi'an Statistics Bureau and Population, 2021), as shown in Table 1. The time to strengthen the interventions can be determined by the timing of important events during the 2021 COVID-19 epidemic in Xi'an city. By using the least squares method, the estimated values of unknown parameters in model (2.1) with (2.2) are listed in Table 1, and the data fitting results are given in Fig.10 (a)-(d). And we can obtain that the initial reproduction number of Xian is 3.72 by using the next generation matrix method. This shows that the simple model can well fit the number of reported cases by the controlled area and the uncontrolled area, providing a model method for evaluating the

Table 1: Definitions and values of variables and parameters for system (2.1) with (2.2).

Parameters	Description	Value-Xi'an	Value-Tibet	Value-Xinjiang	Resource
S_0	Initial value of susceptible population	12952907 [30]	110000 (Estimated)	52000 (Estimated)	-
I_0	Initial value of non-isolated (or untraced) infectious population	2	18	12	Estimated
$S_q(0)$	Initial value of quarantined susceptible population	0	0	0	Data
$I_q(0)$	Initial value of isolated infectious population	0	0	0	Data
H_0	Initial value of hospitalized population	1	22	10	Data
R_0	Initial value of recovered population	0	0	0	Data
β	Transmission probability per contact	0.13675	0.13	0.134	Estimated
c_0	Initial contact rate	10.1317	11.3	8.5	Estimated
c_1	Further reduced contact rate	4.4978	3.368	4	Estimated
φ_0	Initial contact tracing and quarantine rate	0.4524	0.2499	0.249	Estimated
φ_1	Further enhanced contact tracing and quarantine rate	0.7410	0.4201	0.4016	Estimated
δ_I	Diagnosis rate of non-isolated (or untraced) infected individuals	0.1998	0.122	0.219	Estimated
δ_q	Diagnosis rate of isolated infected individuals	0.2001	0.2209	0.13	Estimated
γ_I	Natural recovery rate of infected individuals	0.1006	0.2268	0.1842	Estimated
γ_H	Recovery rate of hospitalized individuals	0.2320	0.3	0.278	Estimated
T_{en}	The time when the control interventions were further strengthened	17	9	14	Data
T_{off}	The time when the control interventions were stopped	-	17	34	Data
R_0	The basic reproduction number at the initial time	3.72	3.16	2.12	Estimated

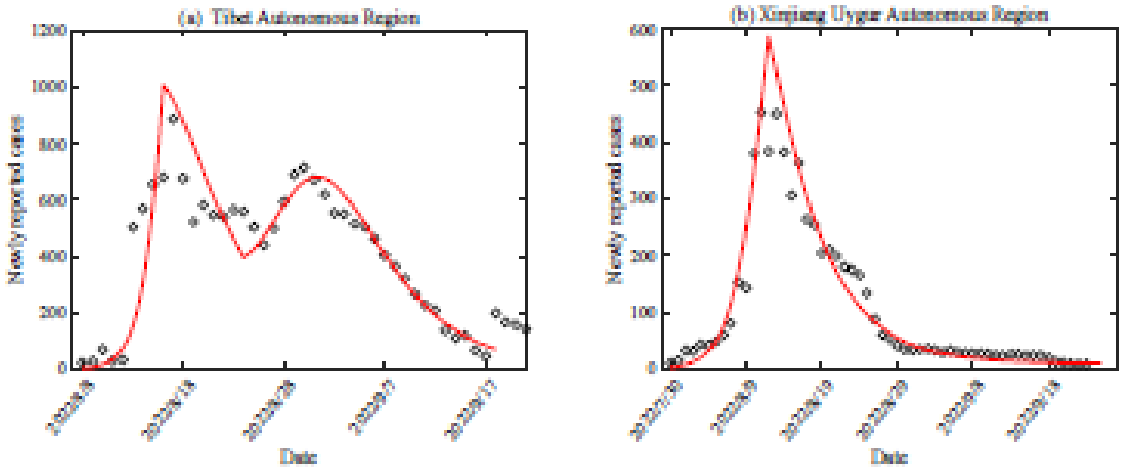

Figure 11: Fitting result of model (2.1) with (2.2) to the epidemic data in the Tibet Autonomous Region and the Xinjiang Uygur Autonomous Region. The black circles represent the reported data, the red curves are the simulation results.

control efficacy.

Note that there are two peaks and a "long tail" of the model output under different interventions and parameter spaces, as shown in Figs.4 and 5, which could also be validated by the epidemics which occurred in the Tibet Autonomous Region and the Xinjiang Uygur Autonomous Region in 2022, China, as shown in Fig.11(a) and (b). The reported COVID-19 cases in Tibet Autonomous Region from 8 August to 17 September have been used to fit the two peaks, and the reported COVID-19 cases in Xinjiang Uygur Autonomous Region from 30 July to 23 September have been used to reveal the fitting of the "long tails" [31, 32]. The various data validations shown in the above further reveal that various characteristics of epidemic evolution can be matched by the dynamic behaviour of the model.

9. Conclusion and Discussion

Understanding the transmission characteristics of infectious diseases in communities, regions and countries can lead to better approaches for mitigating the transmission of emerging infectious diseases. Infectious disease models help us to depict, analyse and reveal the internal mechanism of transmission characteristics [14, 21, 22, 26]. Notably, motivated by the recent COVID-19 outbreak, compartmental models such as the SIR model have been extended to evaluate the efficacy of NPIs on the timing and intensity of epidemics, and optimal strategies have been discussed in the context of minimizing the peak value or final size [15–17]. In order to avoid multiple adverse effects caused by continuous high-intensity NPIs, in this paper, SPCIs have been formulated and introduced into the classical SIR model with a close contact tracing strategy. Further, non-smooth dynamical behaviours have been addressed and analysed aiming to reveal the effects of the timing of SPCIs and the contact tracing strategy on the maximum number of non-isolated infected individuals and the time needed to realize the dynamic zero-case aim. In practice, the model can predict the dynamic evolution of the number of isolated and non-isolated individuals, and present single peak, multi-peak and long tail patterns, which provides a very important model reference for analysing and fitting more than 100 waves of COVID-19 epidemics in China in the past three years.

We initially investigated the peak number of non-isolated infected cases and the time needed to realize the dynamic zero-case aim, and the effects of key parameters including the timing of SPCIs and contact tracing strategy intensity on those two indices (see Figs.4-B.12 and Appendix A). The main results reveal that in order to minimize the maximum number of the non-isolated infected individuals, the optimal time for initiating the SPCIs is when they can control the peak value of a second rebound of the epidemic to be equal to the first peak value. The

impact of the timing of SPCIs and contact tracing strategy on the time needed to realize the dynamic zero-case is complex. Even if the SPCIs are initiated early, this may not shorten the time needed to realize the dynamic zero-case policy. As suggested in Figs.6 and 7, a longer second intervention duration and high quarantine rate are optimal to minimize the time needed to realize the dynamic zero-case aim. When the duration of the second intervention is long enough, the stronger the contact tracing intensity, the more effective they are for shortening the time needed to realize the dynamic zero-case aim.

In particular, we analyzed the impact of SPCIs on the indices concerned, provided important quantitative indices for the design and optimization of SPCI strategies with the goals of minimizing the maximum number of non-isolated infected individuals and the time needed to realize the dynamic zero-case aim. We investigated multi-objective optimal control schemes related to the maximum number of non-isolated infected individuals and the time needed to realize the dynamic zero-case aim numerically. More importantly, the dynamic evolution of the number of isolated and non-isolated individuals, multi-peak and "long tail" patterns have been confirmed by various real data sets of multiple-wave COVID-19 epidemics in China. Note that the "long tail" phenomenon in our model has been verified by the data of the confirmed cases during the COVID-19 epidemic in the Xinjiang Uygur Autonomous Region, China. In this case, the number of infected individuals declined slowly, and it took longer to realize the dynamic zero-case aim even if there were few infected individuals after the second intervention (see Fig.11 (b)). This dynamic behaviour not only provides an important paradigm for the transition from pandemic to endemic under SPCI strategies, it also provides important theoretical support for the adjustment of NPI strategies under the given carrying capacity of medical resources.

Fraser and Steven et al [23] discussed two main factors in controlling the outbreak of an infectious disease (i) isolation of symptomatic individuals and (ii) contact tracing and quarantining of symptomatic individuals. They claimed that asymptomatic infected individuals can affect the spread of the infectious disease and are the critical factor for control. Here we classified asymptomatic infected individuals who are less likely to be detected and difficult to trace as non-isolated infected individuals. The spread of infection outside quarantined areas is mainly caused by non-isolated infected individuals. Removing non-isolated infected individuals are the key in regular epidemic prevention and control, which means realizing the dynamic zero-case policy [24, 25]. We analyzed the effect of SPCIs and close contact tracing strategies on non-isolated infected individuals, and focused on analyzing the dependence of the maximum number of non-isolated infected individuals and the time needed to realize the dynamic zero-case policy on the timing of the second intervention and the intensity of the close contact tracing strategy, and providing quantitative relationships with no approximation. The results of our study further show the importance of the close contact tracing strategy in controlling outbreaks and enrich the results in [15–17, 23].

Our model also has limitations caused by the assumptions we have made to produce a tractable problem. First, compared with the model in [22], we do not consider the exposed individuals (E). It may be difficult to provide the quantitative relationship in a SEIR-type model, which is a very challenging and interesting problem and will be further analyzed in the future. Second, as an idealization, our mathematical model assumes that recovered individuals have complete immunity. Tang and Wang et al [27] collected data from 101 outbreaks in China, where dynamic zeroing for each wave could be achieved in about 40 days. The specific immunity against the virus will rise firstly after infection, and then decline, which provides short-term protection against COVID-19. Therefore, immediate reinfection with the virus is unlikely for a short period [28]. Correspondingly, achieving herd immunity can effectively delay the arrival of the second wave of infection. In practise, the recovered individual may be re-infected again after a long time due to the immunity decline. These complex situations need to be analyzed in detail by introducing the impact of immunity decline into our model. In this case, our model may be not applicable. It may be more applicable to model the short-term spread of infectious diseases (see Fig.10) or those that induce long-term immunity, such as chickenpox and measles. Next, the model is based on a deterministic dynamical system of an isolated population and does not consider interactions among different sub-population and various stochastic influences. A realistic population consists of several sub-population with heterogeneous characteristics. Correspondingly, the interventions can be divided into those that target the entire population at the same time i.e. synchronous interventions) and those that target different sub-population at different times (i.e., asynchronous interventions). These complex situations need to be analyzed in detail by extending the model

proposed to coupled metapopulation models [15, 33] and stochastic epidemic models [34]. Furthermore, our study is a one-shot intervention model, in which the contact and quarantine rates return to the original value after the second intervention. Practically, each new outbreak requires multiple intermittent interventions, making the intervention process much more complex. On the other hand, the contact and quarantine rates in our model change immediately with the intervention. In reality, time delays are prevalent in many controlled systems [35, 36], which make the systematic analysis more complicated and difficult and have a very important impact in the prevention and control of disease. Detailed studies are necessary for the implementation of SPCIs in the complicated real-world environment. We leave this problem as future work.

Data accessibility

The data sets were obtained from the National Health Commission of the People's Republic of China and Province Municipal Health Commissions and are available from their websites (references [30–32], http://sxwjw.shaanxi.gov.cn; http://wjw.xizang.gov.cn; http://wjw.xinjiang.gov.cn.

Authors' contributions

All authors designed and conducted the research. H.Z. and S.T did the theoretical analyses. S.H. and H.Z. did the data analysis and numerical calculations. H.Z., S.T. and R.A.C. were the lead writers of the manuscript.

Competing interests

The authors declare that they have no known competing financial interests or personal relationships that could have appeared to influence the work reported in this paper.

Funding

This work was supported by the National Natural Science Foundation of China (Grant No. 12031010 and No. 12126350). The Fundamental Research Funds for the Central Universities (Grant No. 2021CBLY002).

Appendix A. Analysis of the maximum number of non-isolated infected individuals with respect to T_{on} and T_{off}.

In Theorem 4.1, we summarize the analytical forms of the maximum number of non-isolated infected individuals for cases (a_1)-(a_2) and (a_4)-(a_6) with respect to the number of susceptible individuals at the onset $S_{T_{on}}$ and the end $S_{T_{off}}$ of the second intervention. It follows from the first equation of system (4.1) that $S_{T_{on}}$ and $S_{T_{off}}$ are monotonically decreasing with respect to T_{on} and T_{off}, respectively, i.e. $\frac{\partial S_{T_{on}}}{\partial T_{on}} < 0$ and $\frac{\partial S_{T_{off}}}{\partial T_{off}} < 0$. In the following, we analyse the impact of the start and end timings of the second intervention on the maximum number of non-isolated infected individuals in detail.

(i) **The maximum number of non-isolated infected individuals occurs in the region (a_1), i.e. case (a_1).**

For case (a_1), the maximum number of non-isolated infected individuals is given as

$$I^*_{max} = -\frac{\gamma}{\beta_{10}} + \rho_{10} \ln\left(\frac{\gamma}{\beta_{20}}\right) + \left(\frac{\beta_{20}}{\beta_{10}} - \frac{\beta_{2c}}{\beta_{1c}}\right)(S_{T_{off}} - S_{T_{on}}) + (\rho_{1c} - \rho_{10}) \ln\left(\frac{S_{T_{off}}}{S_{T_{on}}}\right) + \phi_{10}, \tag{A.1}$$

which depends on $S_{T_{on}}$ and $S_{T_{off}}$. It implies that I^c_{max} depends not only on T_{on} but also on T_{off}. Taking the derivative of equation (A.1) with respect to T_{off}, yields

$$\frac{\partial I^c_{max}}{\partial T_{off}} = \gamma I_{T_{off}} \left[R_{e2}(T_{off}) - 1\right] - \frac{\beta_{1c}\gamma I_{T_{off}}(R_{03}-1)}{\beta_{10}} \leq \frac{(\beta_{10}-\beta_{1c})(R_{03}-1)\gamma I_{T_{off}}}{\beta_{10}}. \tag{A.2}$$

Correspondingly, taking the derivative of equation (A.1) with respect to $S_{T_{on}}$, yields

$$\frac{\partial I^c_{max}}{\partial T_{on}} = \gamma I_{T_{on}} \left[R_{e1}(T_{on}) - 1\right] - \frac{\beta_{10}\gamma I_{T_{on}}(R_{02}-1)}{\beta_{1c}} - \left[\frac{\gamma S_{T_{on}} I_{T_{on}}(R_{03}-1)}{S_{T_{off}}} - \frac{\beta_{10}\gamma S_{T_{on}} I_{T_{on}}\left[R_{e2}(T_{off})-1\right]}{\beta_{1c} S_{T_{off}}}\right] \frac{\partial S_{T_{off}}}{\partial S_{T_{on}}}, \tag{A.3}$$

where $\frac{\partial S_{T_{off}}}{\partial S_{T_{on}}} = \frac{\beta_{1c} S_{T_{off}} I_{T_{off}}}{\beta_{10} S_{T_{on}} I_{T_{on}}} > 0$. It follows from equation (A.2) that if $\beta_{1c} > \beta_{10}$, then $\frac{\partial I^c_{max}}{\partial T_{off}} < 0$. Thus, when $\beta_{1c} > \beta_{10}$, I^c_{max} is monotonically decreasing with respect to T_{off}. However, it is difficult to calculate the sign of equation (A.3), so we cannot determine the monotonicity of I^c_{max} with respect to T_{on} for case (a_1).

(*ii*) **The maximum number of non-isolated infected individuals occurs in the region** (a_2)**, i.e. case** (a_2)**.**

For case (a_2), the maximum number of non-isolated infected individuals is given as

$$I^c_{max} = -\frac{\gamma}{\beta_{1c}} + \rho_{11} \ln\left(\frac{\gamma}{\beta_{2c}}\right) + \left(\frac{\beta_{2c}}{\beta_{1c}} - \frac{\beta_{20}}{\beta_{10}}\right) S_{T_{on}} - (\rho_{1c} - \rho_{10}) \ln(S_{T_{on}}) + \phi_{10} \tag{A.4}$$

which only depends on $S_{T_{on}}$. This implies that I^c_{max} only depends on T_{on} for case (a_2). Taking the derivative of equation (A.4) with respect to T_{on}, yields

$$\frac{\partial I^c_{max}}{\partial T_{on}} = \left[\gamma I_{T_{on}} \left[R_{e1}(T_{on}) - 1\right] - \frac{\beta_{10}\gamma I_{T_{on}}(R_{02}-1)}{\beta_{1c}}\right] \geq \frac{(\beta_{1c}-\beta_{10})(R_{02}-1)\gamma I_{T_{on}}}{\beta_{1c}}. \tag{A.5}$$

Thus, if $\beta_{1c} > \beta_{10}$, then $\frac{\partial I^c_{max}}{\partial T_{on}} > 0$. Therefore, when $\beta_{1c} > \beta_{10}$, I^c_{max} is monotonically increasing with respect to T_{on} for case (a_2).

(*iii*) **The maximum number of non-isolated infected individuals occurs in the region** (a_4)**, i.e. case** (a_4)**.**

For case (a_4), the maximum number of non-isolated infected individuals is given as

$$I^c_{max} = -\frac{\beta_{20}}{\beta_{10}} S_{T_{on}} + \rho_{10} \ln(S_{T_{on}}) + \phi_{10} \tag{A.6}$$

which only depends on $S_{T_{on}}$. This implies that I^c_{max} also only depends on T_{on}. Taking the derivative of the above equation (A.6) with respect to T_{on}, we have

$$\frac{\partial I^c_{max}}{\partial T_{on}} = \gamma I_{T_{on}} \left[R_{e1}(T_{on}) - 1\right] > 0. \tag{A.7}$$

Thus, I^c_{max} is monotonically increasing with respect to T_{on} for case (a_4).

(*iv*) **The maximum number of non-isolated infected individuals occurs in the region** (a_3)**, i.e. case** (a_3)**.**

For case (a_3), the maximum number of non-isolated infected individuals is given as

$$I^c_{max} = \{I_1, I_2\}. \tag{A.8}$$

If $I^c_{max} = I_2$, then $\frac{\partial I^c_{max}}{\partial T_{off}} = 0$, and when $\beta_{1c} > \beta_{10}$, $\frac{\partial I^c_{max}}{\partial T_{on}} < 0$. Thus, when $\beta_{1c} > \beta_{10}$, I^c_{max} is monotonically increasing with respect to T_{on}. If $I^c_{max} = I_1$, it follows from equation (A.2) that $\frac{\partial I^c_{max}}{\partial T_{off}} < 0$. Thus, in this case, I^c_{max} is

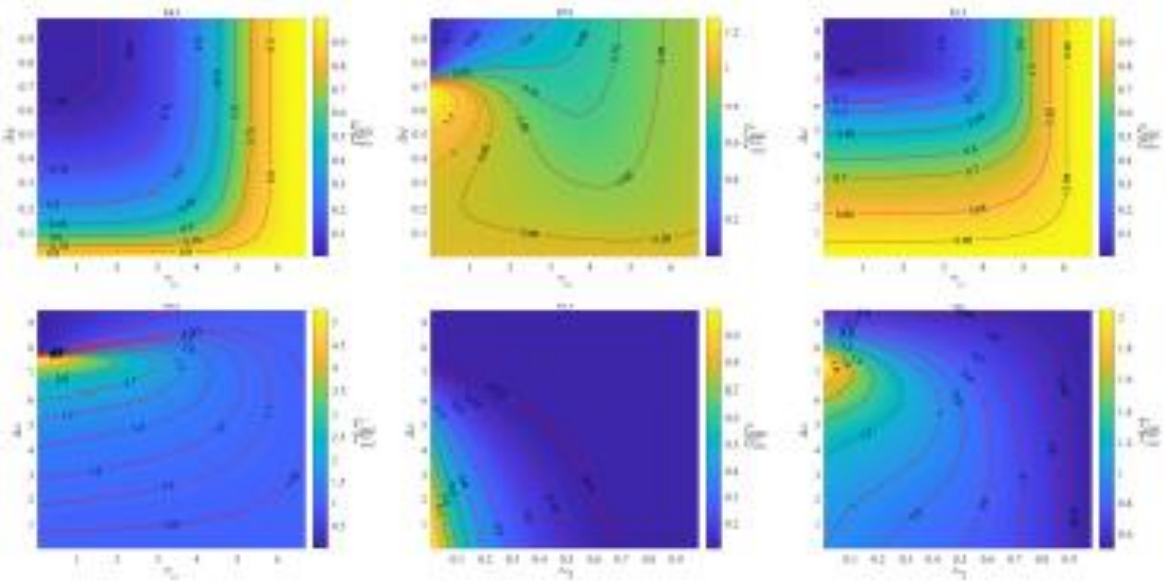

Figure B.12: The impact of the quarantine rate q_c, contact rate c_c and the start time T_{on} of the intervention on the maximum number of non-isolated infected individuals and the time needed to realize the dynamic zero-case aim, where (a) and (b) $c_c = 10$, (c) and (d) $q_c = 0.01526$, (e) and (f) $T_{on} = 3$. Other parameters are as follows: $N = 763$, $S_0 = 762$, $I_0 = 1$, $\beta = 0.155$, $c_0 = 10$, $q_0 = 0.01526$, $\gamma = 0.1$ and $\delta_I = 0.2504$.

monotonically decreasing with respect to T_{off}. Therefore, for case (a_5), $\frac{\partial I^c_{max}}{\partial T_{off}} \leq 0$ and I^c_{max} is quasi-monotonically decreasing with respect to T_{off}. However, it is difficult to calculate the value of equation (A.3), and we cannot determine the monotonicity of I^c_{max} with respect to T_{on} for case (a_5).

(v) **The maximum number of non-isolated infected individuals occurs in the region (a_6), i.e. case (a_6).**

For case (a_6), the maximum number of non-isolated infected individuals is given as

$$I^c_{max} = \{I_{T_{on}}, I_1\}. \tag{A.9}$$

If $I^c_{max} = I_{T_{on}}$, then $\frac{\partial I^c_{max}}{\partial T_{on}} > 0$ and $\frac{\partial I^c_{max}}{\partial T_{off}} = 0$. Thus, I^c_{max} is monotonically increasing with respect to T_{on}. If $I^c_{max} = I_1$, it follows from equation (A.2) that $\frac{\partial I^c_{max}}{\partial T_{off}} < 0$. Thus, in this case, I^c_{max} is monotonically decreasing with respect to T_{off}. Therefore, $\frac{\partial I^c_{max}}{\partial T_{off}} \leq 0$ and I^c_{max} is quasi-monotonically decreasing with respect to T_{off} for case (a_6). However, it is difficult to calculate the sign of equation (A.3), so we cannot determine the monotonicity of I^c_{max} with respect to T_{on} for case (a_6)

Appendix B. Analysis of the special case $T_{off} = T^c_{end}$ in model (2.1) with (2.2).

In the following, we carry out the numerical analyses to understand the effect of the timing of the second intervention and close contact tracing strategy on the maximum number of non-isolated infected individuals and the time needed to realize the dynamic zero-case aim. Here we let $N = 763$, $S_0 = 762$, $I_0 = 1$, $\beta = 0.155$, $c_0 = 10$, $q_0 = 0.01526$, $\gamma = 0.1$ and $\delta_I = 0.2504$, and produce the contour plots of the maximum number of non-isolated infected individuals, and the time needed to realize the dynamic zero-case with respect to T_{on} and Δq, T_{on} and Δc, Δq and Δc, respectively, as shown in Fig.B.12 (a)-(f). In Fig.B.12 (a) and (b), we let $c_c = 10$, i.e. the contact rate during the second intervention is the same as that without the second intervention. It follows from Fig.B.12 (a) that the earlier the second intervention, the stronger the contact tracking intensity during the second intervention,

the smaller the maximum number of non-isolated infected individuals. In Fig.B.12 (b), it is worth mentioning that T^c_{end} is non-monotonically dependent on Δq for a fixed small T_{on}, which implies that even if a second intervention is implemented early, it may take longer to realize the dynamic zero-case policy due to the contact tracing intensity not being strong enough. Therefore, in this case, to minimize the maximum number of non-isolated infected individuals and shorten the duration, the best strategy is to intervene early and fully strengthen the contact tracing intensity. As shown in Fig.B.12 (a) and (b), it is clear that when $(T_{on}, \Delta q)$ nears the point $(1, 0.85)$, both I^c_{max} and T^c_{end} are minimized.

Comparing this with the results shown in Fig.B.12 (a), we can conclude that the contact rate should be reduced to a very low level to get the same I^c_{max} in Fig.B.12 (c). This implies that strengthening the contact tracing intensity is more effective than reducing the contact rate in minimizing the maximum number of infected individuals. It follows from Fig.B.12 (b) and (d) that strengthening the contact tracing intensity is also more effective than reducing the contact rate in shortening the time needed to realize the dynamic zero-case aim.

The results from Fig.B.12 (e) with $T_{on} = 3$ reveal that the stronger the contact tracing intensity, the smaller the contact rate during the second intervention, the more effective they are to minimize the maximum number of non-isolated infected individuals. In terms of the time needed to realize the dynamic zero-case aim, it follows from Fig.B.12 (f) that T^c_{end} is monotonically decreasing with respect to Δq for any fixed Δc. It is worth mentioning that for small and intermediate Δq, T^c_{end} is an upward function of Δc. This means that when the quarantine rate (q_c) is not large enough, in order to shorten the time needed to realize the dynamic zero-case aim, it is necessary to reduce the contact rate to a very low level (i.e. Δc is large enough).

References

[1] P. Zhou, X. Yang, et al, A pneumonia outbreak associated with a new coronavirus of probable bat origin, Nature 579 (2020) 270–273.

[2] F. Wu, S. Zhao, et al, A new coronavirus associated with human respiratory disease in China, Nature 579 (2020) 265–269.

[3] W. Zhang, L. Huang, et al, Vaccine booster efficiently inhibits entry of SARS-CoV-2 omicron variant, Cellular & Molecular Immunology 19 (3) (2022) 445–446.

[4] G. Onishchenko, T. Sizikova, et al, The Omicron Variant of the Sars-Cov-2 Virus As the Dominant Agent of a New Risk of Disease amid the COVID-19 Pandemic, Herald of the Russian Academy of Sciences 92 (2022) 381–391.

[5] X. Wang, X. Zhang, et al, Challenges to the system of reserve medical supplies for public health emergencies: reflections on the outbreak of the severe acute respiratory syndrome coronavirus 2 (SARS-CoV-2) epidemic in China, Bioscience Trends 14 (1) (2020) 3–8.

[6] Y. Ji, Z. Ma, et al, Potential association between COVID-19 mortality and healthcare resource availability, Lancet Global Health 8 (4) (2020) 480.

[7] E. Julia, L. Nicole, et al, Non-pharmaceutical public health interventions for pandemic influenza: an evaluation of the evidence base, BMC Public Health 7 (1) (2007) 208.

[8] N. Ferguson, D. Laydon, et al, Impact of non-pharmaceutical interventions (NPIs) to reduce COVID19 mortality and healthcare demand (Imperial College COVID-19 Response Team, 2020).

[9] S. Flaxman, S. Mishra, et al, Report 13: Estimating the number of infections and the impact of non-pharmaceutical interventions on COVID-19 in 11 European countries (Imperial College COVID-19 Response Team, 2020).

[10] W. H. O. W. Group, Nonpharmaceutical interventions for pandemic influenza, national and community measures, Emerging Infectious Diseases 12 (1) (2006) 88–94.

[11] M. Nicola, Z. Alsafi, et al, The socio-economic implications of the coronavirus pandemic (COVID-19): A review, International Journal of Surgery 78 (2020) 185–193.

[12] T. Rawson, T. Brewer, et al, How and When to End the COVID-19 Lockdown: An Optimization Approach, Frontiers in Public Health 8 (2020) 262.

[13] A. Morgan, M. Woolhouse, et al, Optimizing time-limited non-pharmaceutical interventions for COVID-19 outbreak control, Philosophical Transactions of the Royal Society B 376 (1829) (2021) 20200282.

[14] W. Zhou, Y. Bai, et al, The effectiveness of various control strategies: An insight from a comparison modelling study, Journal of Theoretical Biology 549 (2022) 111205.

[15] F. Lauro, I. Kiss, et alr, Optimal timing of one-shot interventions for epidemic control, Plos Computational Biology 17 (3) (2021) 1–25.

[16] M. Bootsma, N. Ferguson, The effect of public health measures on the 1918 influenza pandemic in U.S. cities, Proceedings of the National Academy of Sciences 104 (18) (2007) 7588–7593.

[17] N. Fujiwara, T. Onaga, et al, Analytical estimation of maximum fraction of infected individuals with one-shot non-pharmaceutical intervention in a hybrid epidemic model, BMC Infectious Diseases 22 (1) (2022) 1–11.

[18] K. Eames, Contact tracing strategies in heterogeneous populations, Epidemiology & Infection 135 (3) (2007) 443–454.

[19] T. Fetzer, T. Graeber, Measuring the scientific effectiveness of contact tracing: Evidence from a natural experiment, Proceedings of the National Academy of Sciences 118 (33) (2021) 1–4.

[20] J. Zu, M. Li, et al, Transmission patterns of COVID-19 in the mainland of China and the efficacy of different control strategies: a data-and model-driven study, Infectious diseases of poverty 9 (1) (2020) 1–14.

[21] B. Tang, X. Wang, et al, Estimation of the Transmission Risk of the 2019-nCoV and Its Implication for Public Health Interventions, Journal of Clinical Medicine 9 (2) (2020) 1–13.

[22] B. Tang, N. Bragazzi, et al, An updated estimation of the risk of transmission of the novel coronavirus (2019-nCov) , Infectious Disease Modelling 5 (2020) 248–255.

[23] C. Fraser, S.Riley, et al, Factors that make an infectious disease outbreak controllable, Proceedings of the National Academy of Sciences 101 (16) (2004) 6146–6151.

[24] H. Li, H. Zhang, Cost-effectiveness analysis of COVID-19 screening strategy under China's dynamic zero-case policy, Frontiers in Public Health 11 (1829) (2023) 1099116.

[25] Joint Prevention and Control Mechanism of the State Council. COVID-19 Disease Prevention and Control Guideline, 2022. Available from: http://www.gov.cn/xinwen/2022-06/28/content_5698168.htm .

[26] M. J. Keeling, P. Rohani, Modeling infectious diseases in humans and animals, Princeton University Press, 2011.

[27] S. Tang, X. Wang, et al, Threshold conditions for curbing COVID-19 with a dynamic zero-case policy derived from 101 outbreaks in China, BMC Public Health 23 (1) (2023) 1–12.

[28] J. Zhao, Q. Yuan, et al, Antibody responses to SARS-CoV-2 in patients with novel coronavirus disease 2019, Clinical Infectious Diseases 71 (16) (2020) 2027–2034.

[29] R. Corless, G. Gonnet, et al, On the Lambert W function, Advances in Computational Mathematics 5 (1) (1996) 329–359.

[30] Shaanxi Municipal Health Commission, 2022. Available from: http://sxwjw. shaanxi.gov.cn.

[31] Health Commission of Tibet Autonomous Region, 2022. Available from: http://wjw.xizang.gov.cn.

[32] Health Commission of Xinjiang Uygur Autonomous Region, 2022. Available from: http://wjw.xinjiang.gov.cn.

[33] S. Contreras, H. Villavicencio, et al, A multi-group SEIRA model for the spread of COVID-19 among heterogeneous populations, Chaos, Solitons & Fractals 136 (2020) 109925.

[34] M. Noor, A. Raza, et al, Non-standard Computational Analysis of the Stochastic COVID-19 Pandemic Model: An Application of Computational Biology, AEJ-Alexandria Engineering Journal 61 (1) (2022) 619–630.

[35] M. Kretzschmar, G. Rozhnova, et al, Impact of delays on effectiveness of contact tracing strategies for COVID-19: a modelling study, The Lancet Public Health 5 (8) (2020) 452–459.

[36] S. Zhai, G. Luo, et al, Vaccination control of an epidemic model with time delay and its application to COVID-19, Nonlinear Dynamics 106 (2) (2021) 1279–1292.